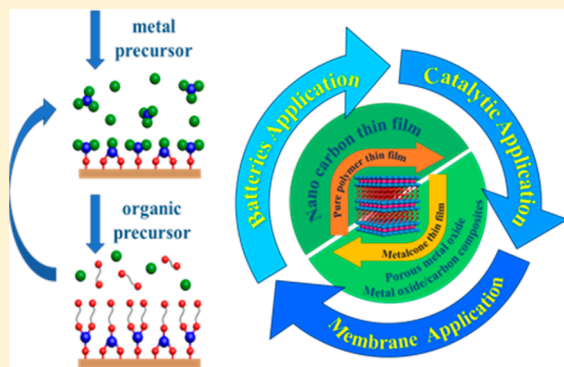


# Molecular Layer Deposition for Energy Conversion and Storage

Yang Zhao<sup>1b</sup> and Xueliang Sun<sup>\*1b</sup>

Department of Mechanical and Materials Engineering, University of Western Ontario, London, Ontario N6A 5B9, Canada

**ABSTRACT:** The development of nanoscale coatings with well-controlled properties is critical to the future of nanotechnology for energy applications. As an extension of atomic layer deposition (ALD), molecular layer deposition (MLD), has recently emerged as a thin-film coating technique that can enable the development of high-performance materials in energy-related applications. MLD fabrication can be classified into two categories: polymer-based organics and inorganic–organic hybrid materials. The unique properties of low growth temperature, precise control of film thickness, uniformity, flexibility, and low density make MLD films very promising for energy-related applications. In this Review, we focus on the recent developments and understanding of MLD in the application of batteries, supercapacitors, water splitting, photodegradation, solar cells, and membranes. The different types of MLD films and nanomaterials derived from MLD are discussed based on the specific application and properties. Finally, the future direction of MLD in energy-related applications has been further investigated.



Organic–inorganic hybrid materials have recently received increasing attention in various areas such as electronics, photonics, and sensing.<sup>1–4</sup> Furthermore, the development of novel hybrid materials at the nanoscale with well-defined properties is critical for high-performance applications, especially in the emerging field of energy-related applications like batteries, supercapacitors, and catalysis.<sup>5–10</sup> Generally, hybrid organic–inorganic materials can inherit advantageous mechanical, optical, chemical, and electrical properties from the combination of organic and inorganic constituents. In this case, the hybrid materials will show synergistic interactions leading to enhanced properties. There are several methods that have been developed to prepare these hybrid materials, including sol–gel methods, Langmuir–Blodgett (LB) techniques, layer-by-layer assembly, self-assembly procedures, etc.<sup>11–13</sup> However, these methods are dependent on solution-based procedures, which face significant challenges in terms of controlling thickness and composition, which are critical parameters for nanoscale applications.

As a novel gas-phase approach, atomic layer deposition (ALD) techniques have been rapidly developed over the past decades. The ALD process is defined as sequential, self-limiting surface reactions that enable the deposition of ultrathin conformal films with atomic-level precision on high aspect ratio structures. The ALD techniques are mainly dependent on binary reaction sequences, which occur on the surface of the substrate. A wide range of binary inorganic compounds, including metal oxides, metal nitrides, metal sulfides, and mixed metal oxides, have been fabricated using simple reactions based on binary systems. Due to the unique properties of ALD, this novel technique has been

widely used in various application areas, and to date, there are several impressive reviews addressing the technique for different applications.<sup>14–17</sup> Figure 1 shows the typical ALD process of  $\text{Al}_2\text{O}_3$ , using trimethylaluminum (TMA) and water ( $\text{H}_2\text{O}$ ) as precursors, which is a well-known procedure in this field.

As an extension of ALD, “molecular” layer deposition (MLD) has been further developed by replacing the oxidizing precursor with organic linkers or the addition of molecular fragments into the film. Figure 1 shows a general schematic representation of MLD growth using sequential, self-limiting surface chemistry. In the 1990s, multiple research groups in Japan developed condensation polymerization reactions for MLD of organic polymers.<sup>18,19</sup> Subsequently, many types of MLD polymer thin films have been studied, such as polyamide, polyimide (PI), polyurea, polyurethane, polythiourea, and polythiolene.<sup>20–28</sup> Alternatively, metal-containing MLD (metalcone) can be accomplished by combining a metal precursor, like  $\text{Al}(\text{CH}_3)_3$ ,  $\text{TiCl}_4$ ,  $\text{SnCl}_4$ , etc., with organic linkers such as those used in MLD for organic polymers.<sup>29–32</sup> Alucones are one of the most widely studied metalcone among the different metal alkoxides. Figure 1 illustrates the reaction mechanism of the first developed alucone using TMA and ethylene glycol (EG) as precursors. As shown in Figure 1, EG molecules contain two hydroxyl groups separated by a carbon chain that serve as reactive linkers for condensation reactions with hydroxyl groups on the metal centers, leading to

Received: January 28, 2018

Accepted: March 6, 2018

Published: March 6, 2018

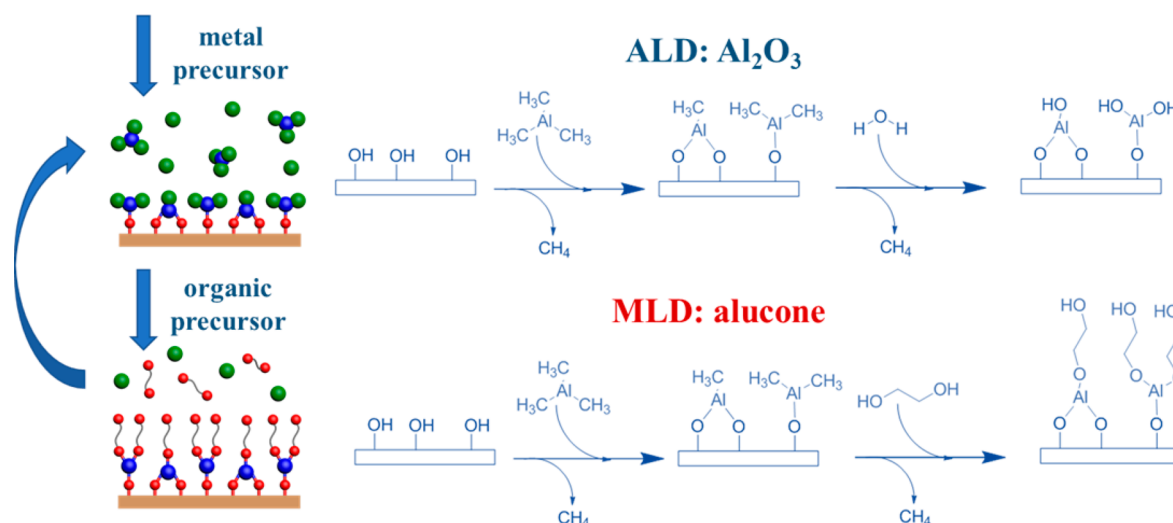


**Figure 1.** Schematic of MLD growth using sequential, self-limiting surface reactions: typical ALD growth mechanism of  $\text{Al}_2\text{O}_3$  using TMA and  $\text{H}_2\text{O}$  as precursors and the MLD growth mechanism of alucone using TMA and EG as precursors.

organic–inorganic hybrid materials. Following the discovery of MLD alucone, several novel metalcones based on different metals (i.e., Zn, Zr, Ti, Hf, Co, Mn, V) and organic molecules (i.e., glycerol (GL), hydroquinone (HQ), hexadiyne diol, polydiacetylene, etc.) have been developed.<sup>33,34</sup> The MLD thin film shows various advantages compared to the ALD thin film due to the organic components in the film: (1) Generally, the ALD metal oxide thin films are relatively brittle, in which defects could be generated under straining in the film. On the contrary, the high flexibility of MLD films would reduce the number and size of defects after straining.<sup>35</sup> Meanwhile, the molecular flexibility will be affected by varying the carbon chain length of organic components in the MLD films (metalcone).<sup>32</sup> (2) The density of MLD thin films is much less than that of ALD metal oxides.<sup>22,36</sup> (3) The MLD thin films, particularly the inorganic–organic metalcone alloy films, display tunable mechanical properties including the density, refractive index, elastic modulus, and hardness by changing the ratios of organic composition.<sup>37</sup> (4) The highly porous metal oxides would be produced by removing the organic components from the MLD (metalcone) thin films using a thermal or chemical process, in which the porosity is tunable by controlling the MLD process.<sup>38</sup> (5) Several types of metalcone alloys show good electrical conductivity and high dielectric constants and refractive indices.<sup>26,37,39,40</sup> However, it still needs to be pointed out that some shortcomings remain for MLD thin films currently. First, the stabilities of some MLD thin films are not satisfactory as most of the EG-based metalcones are sensitive to air and humidity.<sup>5,6,41</sup> Second, the restriction of organic precursors with a sufficient vapor pressure limits the choice for the MLD thin films. Third, porosity of MLD films could lead to diffusion of gas-phase precursors into the polymer, adding a contribution similar to CVD.<sup>22</sup>

Initially, researchers in this field focused on the development and design of new MLD processes to fabricate thin films. A few good reviews have already summarized the growth mechanism, fabrication, and properties of several types of MLD thin films.<sup>5,6,22,41–46</sup> After achieving a better fundamental understanding of this novel technique, MLD technique has been further applied in various applications, including electronically conducting films, sensors, electronic devices, as well as energy storage and conversion.<sup>47–51</sup> However, there are very few review

papers focusing on the utilization of MLD for energy storage and conversion applications. In this Review, we compile a comprehensive summary on the recent development and understanding of MLD in the application of batteries, supercapacitors, catalysis (for water splitting, photodegradation and solar cell), and membranes. The different types of MLD thin films and nanomaterials derived from MLD are discussed in different sections based on the specific applications and properties. Finally, the future direction of MLD in energy-related applications has been further prospected.

**Applications of MLD in Batteries and Supercapacitors.** In the past decades, lithium-ion batteries (LIBs) have become the most widely used energy storage systems for portable electronic devices and electric vehicles due to their desirable properties, which include high energy density, no memory effect, low maintenance, and limited self-discharge.<sup>52–54</sup> The performance of LIBs is mainly dependent on the properties of the electrode materials. Both cathode and anode materials with high specific capacity, appropriate working voltages, and high cycling stability can be considered as ideal candidates. Recently, the fabrication and design of nanostructured electrodes has been widely used as an effective approach to improve the electrochemical performances of LIBs. Nanostructured anodes and cathodes can provide faster electron and lithium-ion transport, improved electrode/electrolyte contact, and are capable of accommodating volumetric strain during discharge/charge processes. Different methods have been carried out to synthesize nanostructure materials, such as sol–gel, solvothermal (hydrothermal), chemical vapor deposition, and wet chemical methods. Another useful route is surface modification or application of thin-film coatings to further enhance the electrochemical performances.<sup>55</sup>

In recent years, ALD has attracted significant attention in the development of batteries and supercapacitors.<sup>56–58</sup> Our previous reviews have summarized the application of ALD for battery technology in detail.<sup>14,59</sup> Recent advancements in ALD have proven to be very promising for battery applications, especially all-solid-state batteries, 2D thin-film batteries, and 3D micro-batteries. In one respect, ALD can be used to directly fabricate electrodes with unique properties of controllable phase, structure, morphologies, particle size, and thickness. Alternatively, surface coating layers fabricated by ALD can significantly improve the specific capacity, cycling stability, rate

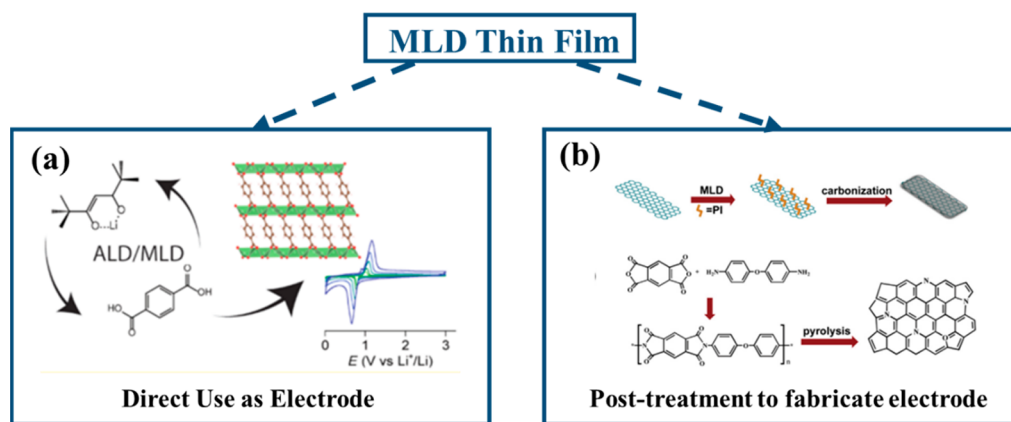


Figure 2. Schematic diagram of MLD thin-film electrodes: (a) direct use as an electrode for batteries or supercapacitors (Copyright American Chemical Society, reproduced with permission from ref 60); (b) post-treatment to fabricate MLD materials as electrodes for batteries or supercapacitors (Copyright Elsevier, reproduced with permission from ref 61).

capability, and thermal stability of the anode and cathode materials. As an extension of ALD, MLD is also considered to be an excellent candidate with unique features for batteries applications. We will discuss the detailed information on MLD for batteries and supercapacitor in the following sections.

**MLD for Synthesis of Electrode Materials.** ALD has been considered as one of the most promising techniques for the fabrication of thin-film electrodes and solid-state electrolytes for batteries and supercapacitors. Early research has been dedicated to the deposition of different types of metal oxide anode/cathode materials on carbon substrates, including  $\text{TiO}_2$ ,  $\text{SnO}_2$ ,  $\text{VO}_x$ ,  $\text{Co}_3\text{O}_4$ , etc.<sup>62–64</sup> Furthermore, complicated cathode and solid-state electrolyte compounds containing multiple elements have been further developed by ALD, including  $\text{LiCoO}_2$ ,  $\text{FePO}_4$ ,  $\text{AlPO}_4$ ,  $\text{LiFePO}_4$ ,  $\text{LiTaO}_3$ ,  $\text{LiPO}_4$ ,  $\text{LiSiO}_x$ ,  $\text{LiNbO}_x$ , etc.<sup>65–71</sup> This approach for the synthesis of metal oxide-based electrodes is a nonaqueous and versatile process that can enable tailored structures, morphologies, and electrochemical properties by tuning the ALD parameters. On the basis of the previous success of ALD in the application of electrode design for batteries and supercapacitors, researchers are exploring the potential of MLD for the similar purposes.

Recently, organic electrode materials have attracted increasing attention as alternatives to the traditional metal-based inorganic electrodes. Organic electrodes possess unique features including low price, environmental friendliness, low weight, as well as relatively high theoretical specific capacities due to the low molecular mass with a possibility for multiple redox processes per molecule. As a promising application, thin-film organic electrode materials can be used for flexible batteries or supercapacitors. In 2016, Karppinen's group first demonstrated the fabrication of lithium terephthalate ( $\text{Li}_2\text{C}_8\text{H}_4\text{O}_4$  or LiTP) as an organic LIB electrode by MLD/ALD (Figure 2a).<sup>60</sup> The as-deposited LiTP organic thin films use  $\text{Li}(\text{thd})$  (thd = 2,2,6,6-tetramethyl-3,5-heptanedionate) and terephthalic acid (benzene-1,4-dicarboxylic acid or TPA) as precursors within the growth temperature range of 200–280 °C. The mechanism of growth was studied by altering the precursor pulse lengths (TPA: 10 s;  $\text{Li}(\text{thd})$ : 4 s) and growth rate at different temperatures ( $\sim 3.0$  Å/cycle at 200 °C), verifying the deposition as a typical MLD process. It is very interesting to note that the LiTP films without any conductive additives can achieve excellent rate capability. Furthermore, with a protective coating layer of solid-state electrolyte (LiPON) by ALD, the LiTP organic electrodes can be stabilized with high

capacity and excellent cycle life. Their study provides new insight toward the development of organic thin-film electrodes for LIBs by MLD. As another popular MLD thin film, titaniconc has also been attempted for use in electrochemical applications.<sup>72</sup> Unfortunately, the titaniconc, using tetrakisdimethylaminotitanium (TDMAT) and GL or EG as precursors, is inactive during cyclic voltammetry (CV). Thus, for this concept, there are still significant challenges for the design of structured MLD thin films with electrochemistry activity.

MLD thin films can be used as templates to fabricate porous carbon or metal oxide films with tunable porosity and heteroatom doping.

Besides the direct use of MLD thin films as electrodes, another effective approach is to use MLD thin films as a template to fabricate nanocomposites via different postdeposition treatments. Metal organic frameworks (MOFs) and covalent organic frameworks (COFs) are some of the hottest materials for energy storage applications and have structures similar to many MLD materials, which also contain metal centers with organic linkers or pure organic connections.<sup>53</sup> Numerous nanomaterials or nanocomposites derived from MOFs or COFs have been reported, including porous carbon, heteroatom-doped carbon, nanostructured metal oxides, and metal oxide/carbon nanocomposites.<sup>53</sup> Following the same post-treatment methods, MLD thin films can act as sacrificial templates to fabricate various types of thin films. On one hand, porous metal oxides, such as  $\text{ZnO}$ ,  $\text{SnO}_2$ ,  $\text{TiO}_2$ , etc., can remain after pyrolysis of the MLD films under air. On the other hand, carbon thin films or metal oxide/carbon nanocomposites will be retained with inert gas flow during the sintering process. Abdulagatov et al. used “titaniconcs (Ti-MLD)” as a template to yield conducting  $\text{TiO}_2$ /carbon composites after pyrolysis under Ar.<sup>73</sup> It was found that the conductivity of the as-prepared thin film increased with increasing pyrolysis temperature, reaching the highest value when heated to 800 °C. Our group also presents a novel way to deposit aluminum alkoxide films with tunable conductivity.<sup>74</sup> The composition of the thin film is tuned by alternating the number of EG and terephthaloyl chloride (TC) cycles between the cycles of TMA and EG. After sintering at different temperatures, a conductive  $\text{Al}_2\text{O}_3$ /carbon composite can be

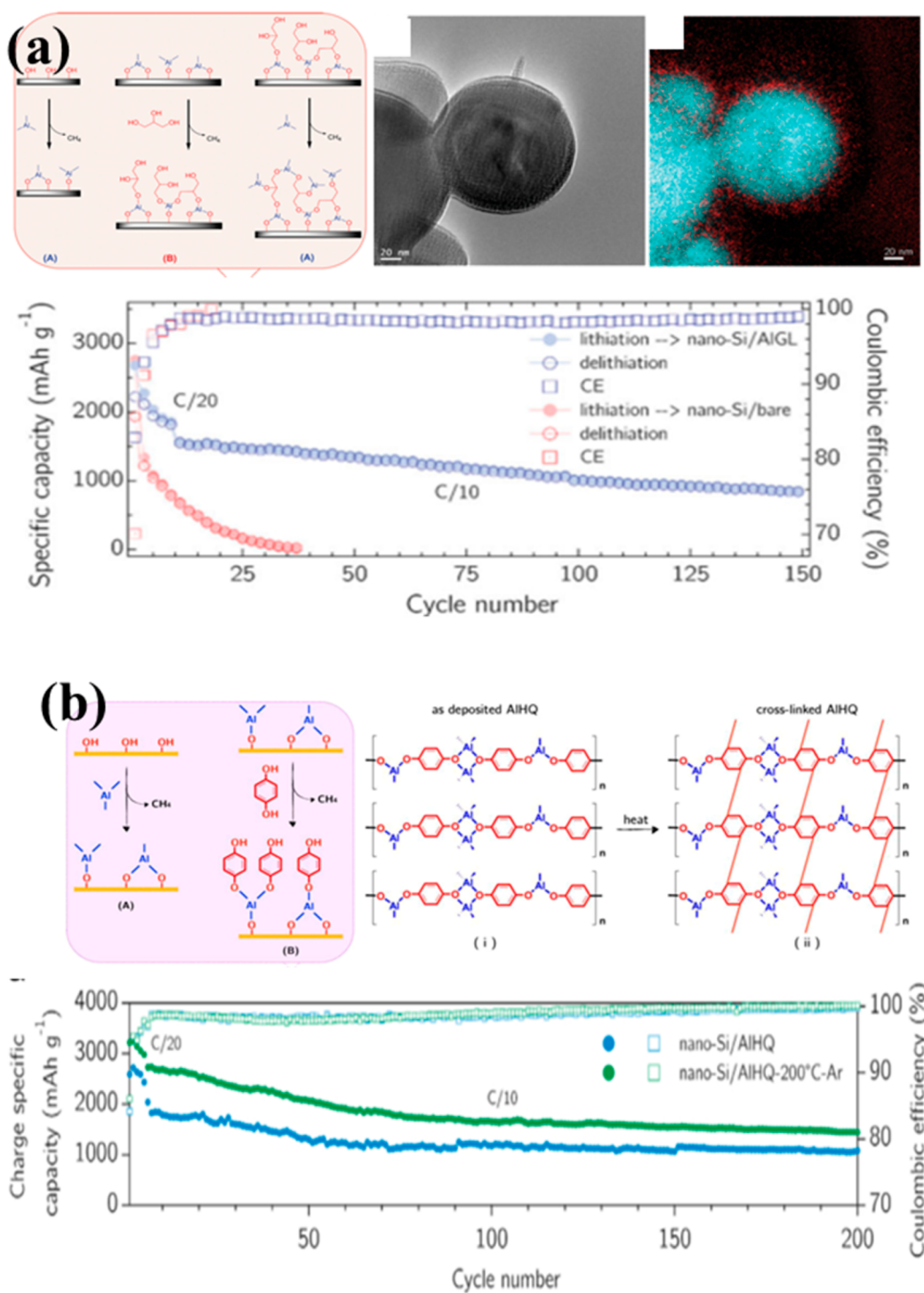


**Figure 3.** (a) Schematic of the self-limiting reactions of Al-GL used to coat the conventional Si nanocomposite electrodes along with TEM images, EELS elements mapping, and cycling performance (Copyright Wiley-VCH Verlag GmbH & Co. KGaA, reproduced with permission from ref 75). The scale bar in the TEM images is 20 nm. (b) Schematic of MLD coating (Al-HQ) and cross-linking processes of the Al-HQ chains after postdeposition heat treatments for the laminated Si electrode. The cyclic capacity and CE of a Si anode coated with as-deposited Al-HQ (blue symbols) is shown and compared to the cyclic capacity and CE of a Si anode coated with Ar-treated Al-HQ (green symbols) (Copyright Elsevier, reproduced with permission from ref 76).

achieved, in which the conductivity of the film is related to the aluminum and carbon ratio.

In order to make a comparison between the ALD-TiO<sub>2</sub> and MLD-derived TiO<sub>2</sub>, Kerckhove et al. carried out different treatments of H<sub>2</sub>O, air, and He for the titanocene thin films.<sup>72</sup> The results show that both samples annealed under air and He

display enhanced rate performances compared with the respective anatase and amorphous TiO<sub>2</sub> references (by ALD). Particularly, the nanocomposites annealed under He had the highest capacity among all treated samples, in which 4.7 times higher capacity (compared to the ALD TiO<sub>2</sub>) can be achieved with a charge current density of 2 mA cm<sup>-1</sup>. This result is an

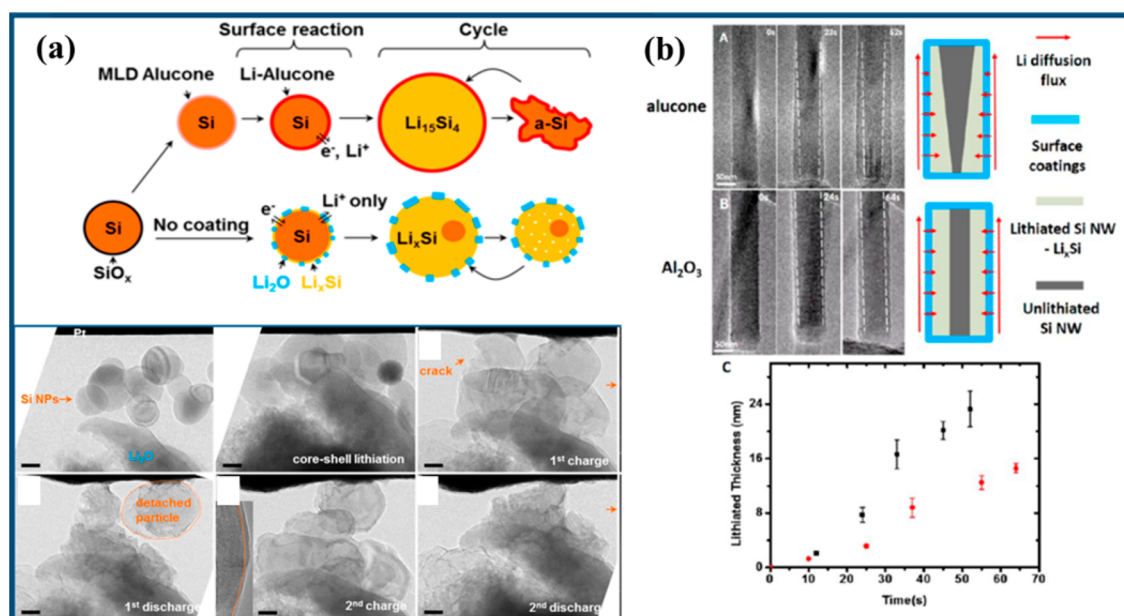


**Figure 4.** (a) Schematics of surface reactions and cycling behavior of silicon nanoparticles with different coating conditions and captured in situ TEM images showing the lithiation/delithiation behavior of the alucone-coated Si nanoparticles (Copyright American Chemical Society, reproduced with permission from ref 85). (b) Time-resolved TEM images show the development of lithiation profiles of the alucone and  $\text{Al}_2\text{O}_3$ -coated SiNWs and schematics of the Li diffusion paths through the SiNWs; average lithiation thickness vs time for the alucone (black square) and  $\text{Al}_2\text{O}_3$  (red dot) coated SiNWs (Copyright American Chemical Society, reproduced with permission from ref 86).

evidence that the inorganic thin film derived from MLD can be more promising than the directly synthesized ALD inorganic thin film. Another interesting work is reported by Qin's group, who produced N-doped carbon-coated graphene by a carbonization process of MLD thin films.<sup>61</sup> The MLD aromatic PI thin film was deposited on a graphene substrate using pyromellitic dianhydride (PMDA) and 4,4'-diaminodiphenyl ether (ODA) as precursors at 160 °C (shown in Figure 2b). After pyrolysis, the N inherited from the precursor can remain to obtain a N-doped carbon coating on graphene. Due to the unique properties of MLD, the PI layers are coated very uniformly on the surface of graphene and enable homogeneous dispersion of nitrogen atoms in the carbonized products. When used as electrode materials for supercapacitors, the nanocomposites exhibit remarkable capacitance performance with a high specific capacitance of 290.2  $\text{F g}^{-1}$  at a current density of 1  $\text{A g}^{-1}$  in 6 M KOH aqueous electrolyte, as well as good rate properties and stability.

To summarize, there are very few reports that focus on the application of MLD thin films as electrode materials for batteries and supercapacitor because the technique is still in its infancy. Many researchers in this field are still concentrating on the development of different types of MLD processes. However, the thin films fabricated by MLD or derived from MLD are very promising for use as electrodes for batteries and supercapacitors.

**MLD Coatings for Battery Materials.** MLD Coatings for Anode Materials. The most common commercialized anode material for LIBs is graphite. However, it suffers from a low theoretical capacity (372  $\text{mAh g}^{-1}$ ) and poor rate properties, which severely limits further improvement in energy density. Si is now considered as one of the most highly investigated anode materials for LIBs due to its high theoretical capacity of 4200  $\text{mAh g}^{-1}$ .<sup>77–79</sup> Regardless of the high capacity, the serious volume change of Si (over ~400%) during Li alloying and dealloy processes leads to pulverization and degradation of Si electrodes. In order to solve this issue, several approaches have been

attempted in previous studies. One of the most popular techniques is to design nanostructure Si with void spaces, including nanowires, core-shell nanowires, and hollow structures to accommodate the volume change. Coating or combining the buffering matrix with Si is another way to relieve the problems associated with volume expansion. Among the various surface coating candidates, the rich chemistry of polymeric materials offers great flexibility, which is ideal for the volume change of Si-based materials.<sup>80–84</sup> MLD thin films can also be considered as buffer layers for Si nanocomposites due to the mechanically robust and flexible nature, which is not evident in ALD metal oxides. D. M. Piper et al. first demonstrated one of the most popular MLD thin films, alucone, as a coating buffer layer for Si nanoparticles.<sup>75</sup> Figure 3a shows a schematic of the self-limiting surface reactions involved in the formation of alucone using TMA and GL as precursors. As a result of the deposition process, the Si nanoparticles are coated with thin and conformal layers of Al-GL, which can be observed from the TEM images and confirmed by EESL mapping (Figure 3a). When tested as an anode material for LIBs, the Si/Al-GL nanocomposites exhibit a high specific capacity of nearly 900  $\text{mAh g}^{-1}$  after 150 cycles, and in contrast, the bare Si nanoparticles show rapid degradation and fail after only 30 cycles. The results indicate that the Al-GL coating provides favorable mechanical properties and flexibility capable of accommodating volumetric expansion of the Si nanoparticles. Afterward, the same group developed a new MLD reaction combining TMA with another aromatic organic diol (HQ), leading to a robust, elastic, and conductive surface coating composed of aluminum dioxybenzene.<sup>76</sup> Figure 3b shows a schematic diagram of the typical MLD process using TMA and HQ as precursors, indicating controlled layered growth. The linear growth rate of Al-HQ is measured to be 7.5  $\text{Å/cycle}$  at a deposition temperature of 150 °C. Interestingly, the Al-HQ thin films are further dehydrogenated when annealing under both inert and air atmosphere. The

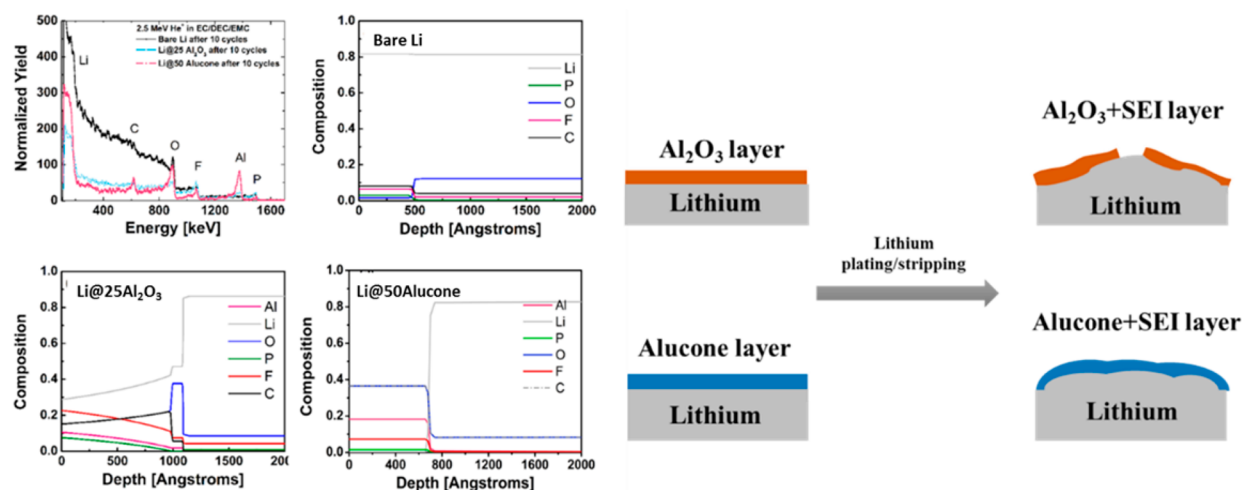


Figure 5. Comparison of RBS spectra for bare Li, Li@25Al<sub>2</sub>O<sub>3</sub>, and Li@50alucone after 10 cycles in EC/DEC/EMC electrolyte; calculated depth profiles and schematic diagrams illustrating morphological changes in the films (Copyright Wiley-VCH Verlag GmbH & Co. KGaA, reproduced with permission from ref 110).

longitudinal cross-linking reaction of aluminum-dioxybenzene chains occurs due to the dehydrogenation. It is believed that the polydentate Lewis acid-enabled cross-linking structure can create strong covalent bonding on the surface of Si nanoparticles as well as provide higher stability due to the film coating, which is shown in Figure 3b. They also confirm that the Al-HQ film with heat treatment at 150 °C has the highest Young's modulus, suggesting a more elastic deformation, which is expected to show less accumulative strains and strain energies. Similar to their first work, the Al-HQ coating layer is uniformly distributed on the Si nanoparticles. With the additional benefits arising from the MLD film, the Al-HQ-coated Si nanoparticles showed enhanced electrochemical performances compared to the pristine Si nanoparticles. After 200 cycles, the Al-HQ-coated (treated at 200 °C) electrodes exhibit a specific capacity of nearly 1500 mAh g<sup>-1</sup> and Coulombic efficiency (CE) in excess of 99%. Furthermore, the as-deposited Al-HQ-coated electrodes show a stable capacity of 1000 mAh g<sup>-1</sup>. Their newly developed MLD coating of Al-HQ has a capacity three times higher than that of the Al-GL thin-film coating. In this case, the postelectrode manufacturing surface modification by MLD is compatible with that of Si-based materials and can be further extended to other high-capacity materials with large volume changes.

In order to obtain a better understanding of the influence of MLD coating on the performances of Si nanoparticles, Ban et al. collaborated with Wang's group to display an in situ TEM analysis on both uncoated and alucone-coated Si nanoparticles.<sup>85,86</sup> The lithiation and delithiation characteristics of the alucone-coated (Al-GL) Si nanoparticles are revealed by sequential TEM images in Figure 4a. Compared with pristine nanoparticles, there is no Li<sub>2</sub>O formed on alucone-coated Si nanoparticles because of the dramatic removal of SiO<sub>x</sub> during the alucone coating process. The results indicate that the alucone-coated Si nanoparticles have fast, thorough, and highly reversible lithiation behaviors, which are clarified to be associated with the mechanical flexibility and fast Li<sup>+</sup> conductivity of the alucone coating. Further studies have been attempted on alucone-coated Si nanowires (SiNWs) by the same group using in situ TEM.<sup>86</sup> They found distinctly different lithiation profiles between alucone and Al<sub>2</sub>O<sub>3</sub>, in which alucone is V-shaped and Al<sub>2</sub>O<sub>3</sub> is H-shaped, respectively, as shown in Figure 4b.

To obtain a deeper understanding of alucone-coated Si nanoparticles, Ma et al. examined the film formation, lithiation, and reactivity in contact with an electrolyte solution using density functional theory, ab initio molecular dynamics simulations, and Green's function theory.<sup>87</sup> It was found that the alucone film is composed of Al–O complexes with 3-O or 4-O coordination. When Li ions are inserted into the film, there is very strong bonding between the Li and O atoms in the energetically favorable sites. Furthermore, the film becomes electronically conductive after the film is irreversibly saturated with Li atoms. The theoretical results are in agreement with those from morphology and electrochemical analysis.

The metallic Li anode has also been strongly considered as an ideal anode material for LIBs, particularly for next-generation Li metal batteries (Li–S, Li–air, all-solid-state battery) due to their high specific capacity (3860 mAh g<sup>-1</sup>), low potential (−3.04 V vs the standard hydrogen electrode), and light weight (0.53 g cm<sup>-3</sup>).<sup>88,89</sup> However, a number of issues, such as dendrite growth and volume change, plague the successful application of lithium metal for practical devices. The constant stripping/plating process of Li in each cycle eventually leads to uneven surface morphologies with mossy or dendritic Li growth and poor CE due to side reactions. In this case, two critical problems arise for Li metal; one is the safety concern over potential internal short circuits, and another is the short cycle life. Furthermore, fire and other hazards may occur as a result of failure of the batteries.<sup>90–94</sup> One of the key components of the metallic Li anode is the formation of a solid electrolyte interphase (SEI) layer, which is formed during the initial charging/discharging processes as a result of reaction between Li metal and different components in the electrolyte. Although the SEI formation will intrinsically consume both Li and the electrolyte leading to a lower CE, it can effectively prevent further contact and reactions with the electrolyte, leading to a stabilized surface. However, the collapse of an unstable SEI film can aggravate local dendrite growth and undesired electrolyte deposition due to nonhomogeneous local current densities. Recently, two different groups demonstrated ultrathin ALD Al<sub>2</sub>O<sub>3</sub> coatings as protective layers for metallic lithium.<sup>95,96</sup> In their results, the ALD Al<sub>2</sub>O<sub>3</sub>-protected Li can prevent Li metal corrosion in electrolyte and reduce dendrite growth, which further enhances electrochemical performance with elevated capacity and longer lifetimes. Due to the toughness

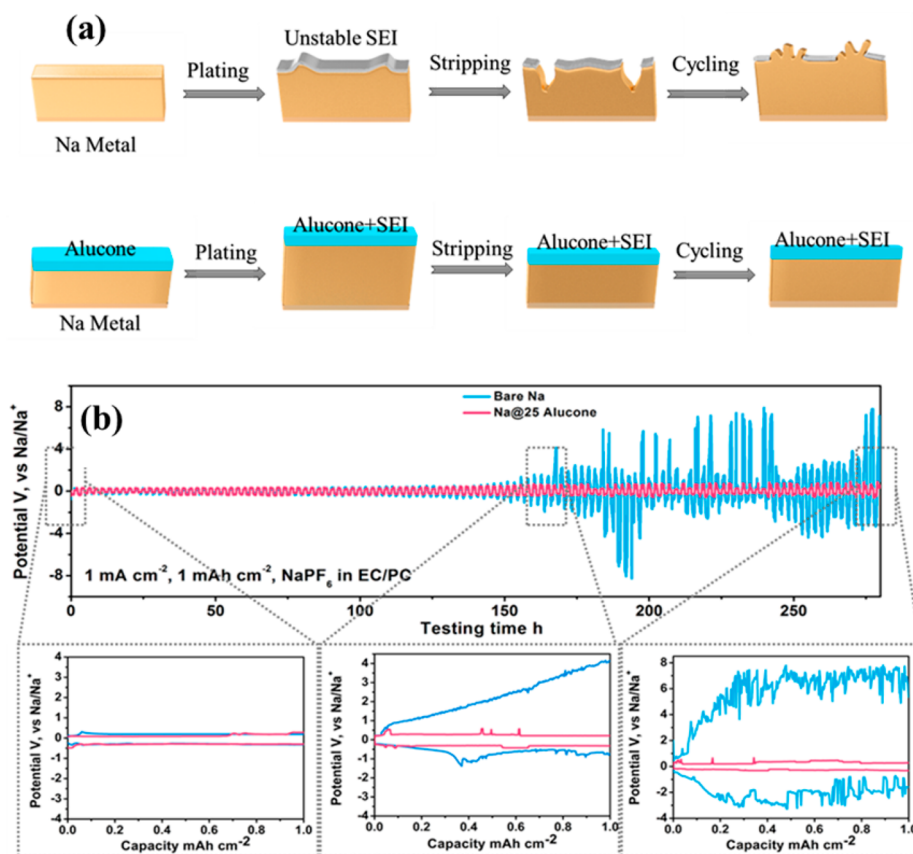


**Figure 6.** (a) Schematic diagrams of Na stripping/plating on bare Na foil and Na foil with MLD alucone coating; (b) comparison of the cycling stability of the Na@25Alucone and the bare Na foil at a current density of  $1 \text{ mA cm}^{-2}$ ; voltage profiles of Na@25Alucone and bare Na foil in the three different stages (Copyright American Chemical Society, reproduced with permission from ref 97).

and flexibility of hybrid inorganic–organic thin films by MLD, our group first demonstrated the use of an ultrathin MLD alucone (Al-EG) coating as a protective layer for metallic Li to achieve an improved lifetime and stability.<sup>110</sup> Our results show that the Al-EG coating layer can stabilize the SEI film and further change the morphology of lithium growth during the plating/stripping process. Meanwhile, the MLD coating layer can greatly improve the stability in both ether-based (used in Li–S batteries) and carbonate-based (used in LIBs) electrolytes, which is more promising compared with the ALD  $\text{Al}_2\text{O}_3$  coating. In order to elucidate compositional changes following the plating/stripping cycling experiments, Rutherford backscattering spectrometry (RBS) measurements were performed for all samples (shown in Figure 5). While bare Li shows significant oxidation and penetration of P and F from the electrolyte into subsurface layers,  $\text{Al}_2\text{O}_3$  and alucone films act as good protective barriers, with small concentrations of P, F, and C localized in the first 70–100 nm from the surface. Notably, the Li@50 alucone film mostly remains as a continuous film during cycling, as is evident from the relatively sharp Al, O, and C peaks, and very small changes in composition compared to an as-deposited alucone film. It is believed that our design of MLD alucone-coated Li anodes opens up new opportunities for the realization of next-generation high energy density Li metal batteries.

Beyond LIBs, Na-ion batteries (NIBs) and Na metal batteries (NMBs, including Na–S and Na– $\text{O}_2$  batteries) have been explored as alternatives to the traditional LIBs due to the wide availability and low cost of sodium. Among the various anode materials for NIBs and NMBs, Na metal is the most promising

candidate due to the low redox potential and high theoretical specific capacity of  $1166 \text{ mAh g}^{-1}$ . However, Na metal suffers from similar issues existing with Li metal anodes, including the unstable SEI layer of nonuniform ionic flux and mossy or dendritic growth of Na during repetitive stripping/plating processes (Figure 6a). Our group and Hu's group have reported protective coatings of ALD/plasma enhanced ALD (PEALD)  $\text{Al}_2\text{O}_3$  on Na metal anodes in two types of electrolyte ( $\text{NaSO}_3\text{CF}_3$  in DEGDME and  $\text{NaClO}_4$  in EC/DEC).<sup>98,99</sup> Both works show that the ALD  $\text{Al}_2\text{O}_3$  coating can obtain superior stable performances and improved lifetime for Na metal anodes as well as reduced dendrite growth. Furthermore, our group successfully demonstrated the application of alucone (Al-EG) as a protective layer for Na metal in the  $\text{NaPF}_6$  in EC/PC electrolyte system.<sup>97</sup> Compared with bare Na, Na@25Alucone shows significantly enhanced electrochemical stripping/plating performances under different current densities. Meanwhile, the application of 25 MLD cycles of alucone leads to a smoother Na metal surface after plating, and Na dendrite growth is effectively reduced (Figure 6). Furthermore, MLD alucone protecting Na metal shows better performances compared with ALD  $\text{Al}_2\text{O}_3$ -coated Na in  $\text{NaPF}_6$  (EC/PC) electrolyte.

MLD thin films with high flexibility and toughness can relieve volume expansion for the Si anode.

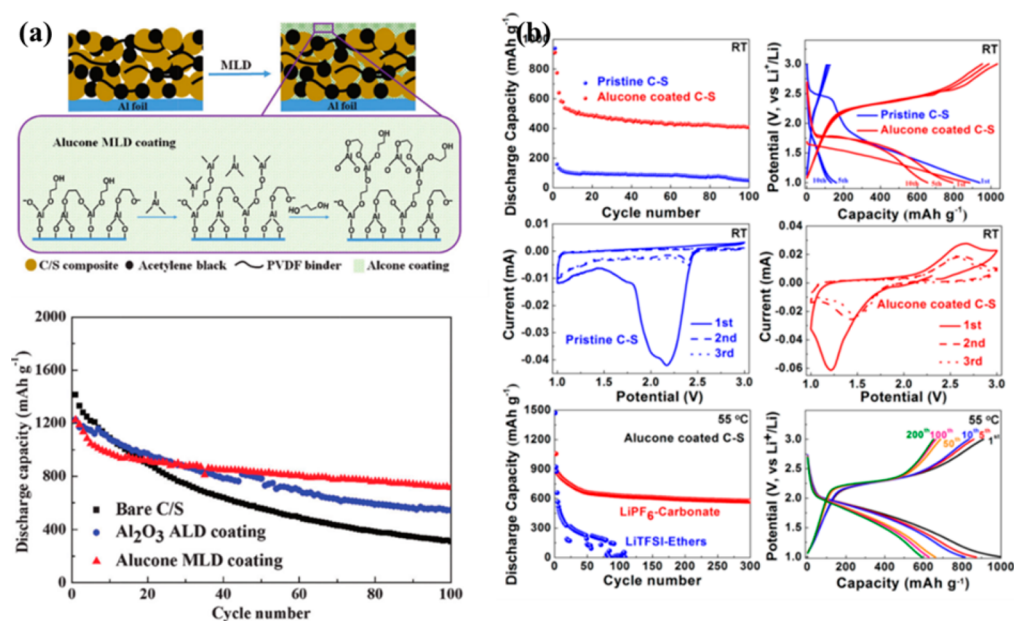


Figure 7. (a) Schematic of alucone MLD thin-film formation as a coating layer applied on a C/S cathode; cycle performances of bare, ALD-Al<sub>2</sub>O<sub>3</sub>-coated, and MLD alucone-coated C/S cathodes at a current density of 160 mA g<sup>-1</sup> (Copyright Royal Society of Chemistry, reproduced with permission from ref 100). (b) Electrochemical cycle performance, discharge–charge profiles, CV profiles of alucone-coated and pristine C/S electrode, and comparison of alucone-coated C/S electrodes running within carbonate-based and ether-based electrolytes under 55 °C (Copyright American Chemical Society, reproduced with permission from ref 101).

Briefly, the MLD thin films show very promising potential for surface modifications of the anode materials in LIBs. The roles of MLD coating for addressing the challenges for anodes can be divided into three parts: (1) During electrochemical cycling, a thin MLD film can transfer from nonionic conductive into ionic conductive for Li<sup>+</sup> ion transport; (2) the high flexibility and toughness of the MLD thin film can effectively relieve the large volume change for the alloy-based anode materials; and 3) the MLD thin film can be considered as an artificial SEI layer or stabilize SEI formation to reduce dendrite growth for the alkali metal anode.

MLD Coatings for Cathode Materials. Li sulfur batteries, as one of the most promising next-generation battery systems, have been intensively studied because of their high theoretical capacity and energy density. However, the so-called “shuttle effect”, which is caused by the dissolution of polysulfides, leads to rapid decay in electrochemical performance and CE. Furthermore, low conductivity and large volume expansion of sulfur are other significant problems for Li–S batteries. In order to solve these issues, surface coating with carbon or metal oxides has proven to be an effective approach to prevent the shuttle effect and accommodate the large volume expansion. In our earlier work, we studied the coating of sulfur-based electrodes with Al<sub>2</sub>O<sub>3</sub> coatings of varying thickness.<sup>102</sup> Our results showed that two cycles of ALD Al<sub>2</sub>O<sub>3</sub> (~0.2 nm) yield the best performance of Li–S batteries. It was found that an ionically conductive layer of AlF<sub>3</sub>/LiAlO<sub>2</sub> is formed during the lithiation process of the surface coating. This ionic conductive layer cannot only protect the dissolution of polysulfide but also enhance the Li-ion diffusion, resulting in highly reversible electrochemical performances. Subsequently, we demonstrated that an alucone (Al-EG) thin-film coating directly on the sulfur cathode can significantly improve the cycling stability and capability of Li–S batteries (shown in Figure 7a).<sup>100</sup> The thickness of the alucone coating has been optimized and investigated for electrochemical performances with 2, 5, 10, and 20 MLD cycles on the surface of sulfur

electrodes. Different from the Al<sub>2</sub>O<sub>3</sub> coating layers, all of the alucone-coated electrodes show effective enhancement in stability and CE, in which five cycles of alucone coating delivers the highest specific discharge capacity of 710 mAh g<sup>-1</sup> after 100 cycles and stable CE of over 90%. When compared to previous ALD-Al<sub>2</sub>O<sub>3</sub> coatings, MLD alucone shows superior electrochemical performances, which is shown in Figure 7a. The morphologies of the pristine electrode and alucone-coated electrode have been examined before and after electrochemical cycling by SEM. The SEM results indicate that the pristine electrode is totally covered with discharge products after cycling; however, the alucone coating can effectively inhibit discharge product deposition on the surface. It is believed that the reduced dissolution of polysulfide and good mechanical properties of the alucone coating lead to highly improved electrochemical performances for C/S cathodes.

During our research of alucone-coated C/S electrodes, a more interesting phenomenon has been further explored and revealed in our latest report.<sup>101</sup> We found that alucone-coated C/S electrodes cannot only display a high specific capacity in ether-based Li–S electrolyte (LiTFSI in DOL/DME) but also can be used in traditional carbonate-based Li-ion electrolyte (LiPF<sub>6</sub> in EC/DEC/EMC), which has not been realized before. Furthermore, cycling can also be carried out at high temperature with ultralong cycle life and stability. Figure 7b shows the electrochemical performances, in which the alucone-coated electrode delivers an initial capacity of 912 mAh g<sup>-1</sup> and stabilizes at 429 mAh g<sup>-1</sup> after 100 cycles. However, the bare C/S electrode drops to 159 mAh g<sup>-1</sup>, indicating the occurrence of irreversible electrochemical processes. Meanwhile, the alucone-coated C/S electrode displays well-defined plateaus during discharge/charge processes and reproducible cathodic/anodic peaks in the CV curves. To demonstrate the electrochemical performances of high-temperature Li–S batteries, the alucone-coated C/S electrode has been tested with both ether-based and carbonated-based electrolyte at 55 °C. Impressively, alucone-

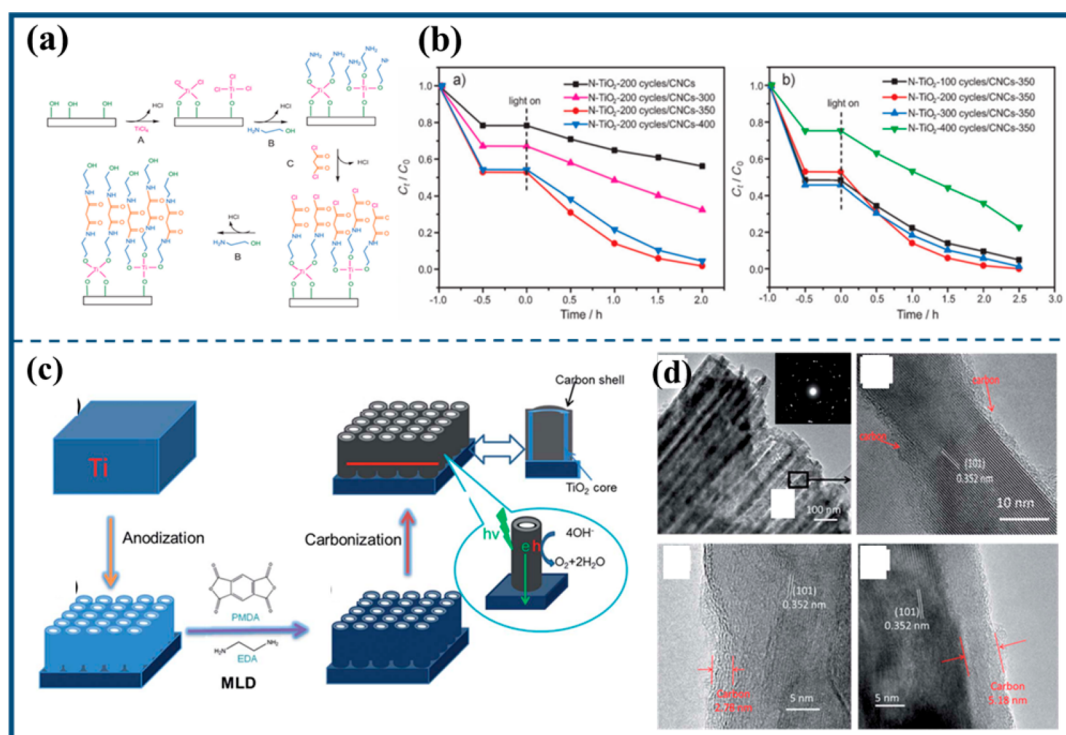


**Figure 8.** (a) Four-step ABCB reaction sequence for Ti-hybrid film formation using TiCl<sub>4</sub>, EA, and MC as molecular precursors. (b) Photocatalytic degradation of MB under visible light irradiation monitored as the normalized concentration change versus irradiation time for different samples (Copyright Wiley-VCH Verlag GmbH & Co. KGaA, reproduced with permission from ref 38). (c) Schematic illustration of the coating of TNTAs with an ultrathin carbon film. (d) TEM image of a TNTA-coated carbon film; onset potential measurement for the oxygen evolution reaction (OER) (Copyright Royal Society of Chemistry, reproduced with permission from ref 103).

coated C/S electrodes demonstrate improved capacity and extended cycle life in Li–S batteries using carbonate-based electrolyte. The capacity of the alucone-coated electrode remains at 661 mAh g<sup>-1</sup> after 50 cycles with a capacity retention of 573 mAh g<sup>-1</sup> after 300 cycles. The controllable nature of MLD enables the use of conventional carbon–sulfur cathode materials in traditional carbonate-based electrolyte for Li–S batteries and provides a facile and versatile method that can be applied to a variety of C/S electrodes without redesigning the carbon host materials.

In this section, the recent development of MLD in the application of energy storage (batteries and supercapacitors) has been summarized in detail. Briefly, the MLD thin film can be used for energy storage applications in terms of three approaches: (1) directly use MLD thin films as electrodes; (2) nanocomposites derived from MLD thin films; (3) surface modification by MLD thin films. However, there are only a few reports for MLD thin films in the applications of batteries and supercapacitors and MLD has already shown promising potentials in these areas. These further efforts will continue to build better design and wider application of MLD thin films for battery and supercapacitor applications, leading to high-performance, long-lifetime energy storage devices.

**MLD in Catalytic Applications.** As one of the most important semiconductors, TiO<sub>2</sub> has been widely used as a catalyst in many different applications, including solar energy devices, environmental remediation, and as a catalyst support. ALD TiO<sub>2</sub> with a controllable phase, structure, morphologies, and thickness is now a well-known and typical process using TiCl<sub>4</sub> and H<sub>2</sub>O as precursors. However, the TiO<sub>2</sub> films deposited by ALD are intrinsically pinhole-free with low specific surface areas, resulting

in low catalytic activity. Ishchuk et al. presented the design and transformation of MLD titanocene films (Ti-EG) into highly active photocatalytic films.<sup>104</sup> The photocatalytic activities of the films are investigated using hydroxyl-functionalized porphyrin as a spectroscopic marker. The different annealing temperatures for the Ti-EG film are investigated for the photocatalytic activity as well as the TiO<sub>2</sub> films prepared by ALD. Their results show that the photocatalytic activity of the annealed MLD Ti-EG thin film for optimal process conditions is about 5 times higher compared to that of the ALD TiO<sub>2</sub> thin film. The results demonstrate the relationship between structure and photocatalytic activity, in which the intermediate film state with both crystalline and amorphous regions shows high dye loading and high catalytic activity. In contrast, the films with either an amorphous state or highly crystalline state present low photocatalytic activity. Their results demonstrate the feasibility and potential of MLD to form metal oxides with high photocatalytic activity. Furthermore, Qin's group designed a new MLD process for the fabrication of porous N-doped TiO<sub>2</sub> films.<sup>38</sup> Figure 8a shows the four-step ABCB MLD reaction sequence for Ti-hybrid film formation using TiCl<sub>4</sub>, ethanolamine (EA), and malonyl chloride (MC) as molecular precursors. After post-treatment annealing in a H<sub>2</sub>/Ar atmosphere, N-doped TiO<sub>2</sub> nanoporous films can be obtained from the deposited Ti-hybrid MLD films. The distance between the adjacent Ti moieties can be controlled by tuning the length of organic linkers during the MLD process. The photocatalytic activities of as-prepared porous N-doped TiO<sub>2</sub> CNCs with different numbers of MLD cycles were evaluated through the photodegradation of methylene blue (MB) under visible-light irradiation, and the preliminary results are shown in Figure 8b. It can be clearly seen that samples annealed at 350 °C deliver the

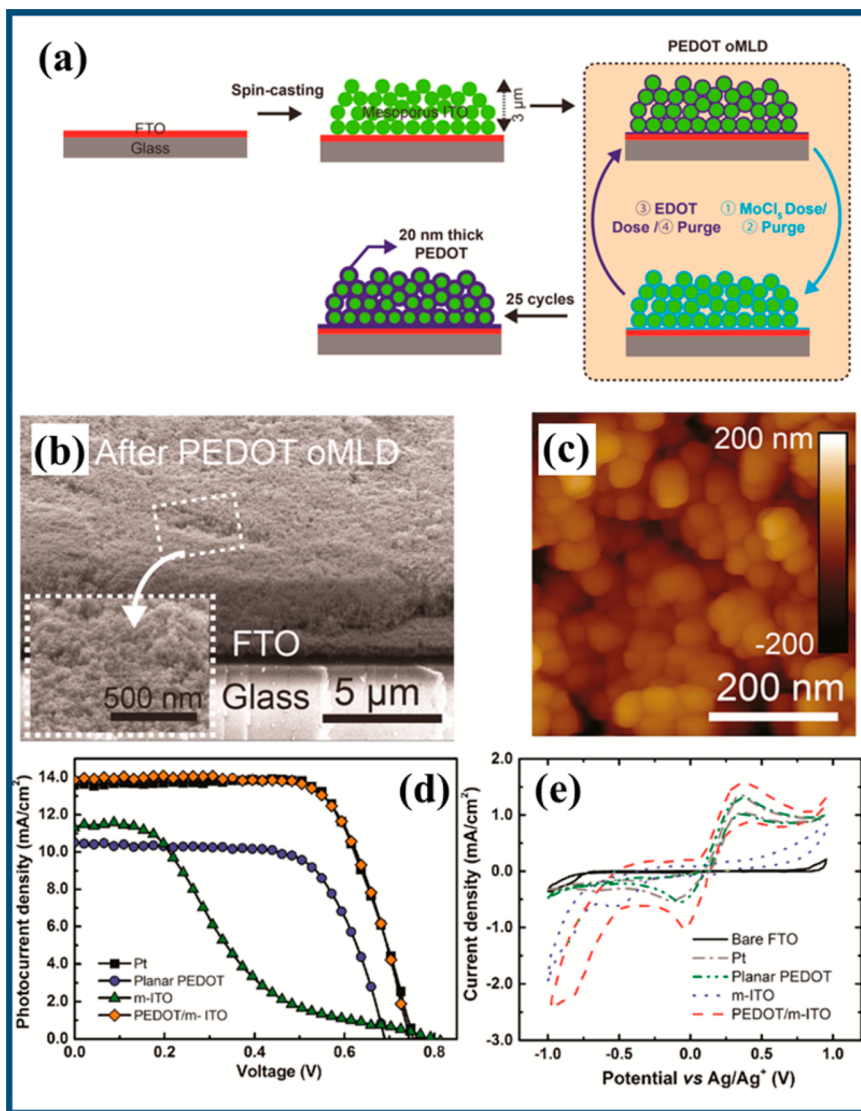


Figure 9. (a) Process scheme for fabricating PEDOT-coated m-ITO films for a cathode in DSSCs using oMLD; (b) tilted-view SEM image of PEDOT-coated m-ITO on FTO glass in which the inset presents the top surface in the dotted box; (c) AFM image of  $\sim 20$  nm thick PEDOT-coated m-ITO; (d) photovoltaic performance of representative DSSCs assembled with four different CEs; (e) CV obtained after 10 cycles with four CEs in electrolyte containing 10 mM LiI, 1 mM  $I_2$ , and 0.1 M  $LiClO_4$  acetonitrile solution at a scan rate  $20 \text{ mV}^{-1}$  (Copyright American Chemical Society, reproduced with permission from ref 106).

best performances. This result can be rationalized by the higher surface area after removal of amorphous carbon and less aggregation of  $TiO_2$  at relatively lower temperatures. The thickness effect of MLD is also revealed, in which the N-doped  $TiO_2$ /CNCs with 200 MLD cycles indicated the fastest decomposition rate for MB, which can be attributed to the synergy of  $TiO_2$  and shorter diffusion path length in correlation with the MLD film thickness.

Qin's group also demonstrated another way to further enhance the photoelectrochemical water splitting performances by utilizing  $TiO_2$  nanotube arrays.<sup>103</sup> Figure 8c presents the design and fabrication process of the thin carbon-coated  $TiO_2$  nanotube arrays. Generally, the  $TiO_2$  nanotube arrays are obtained by the electrochemically anodized method, and the MLD process uses PMDA and ethylenediamine (EDA) as precursors. The TEM images of the carbon-coated  $TiO_2$  nanotube arrays are shown in Figure 8d. It can be seen that the ultrathin N-doped carbon film can be produced after the annealing process under Ar with the concurrent conversion of  $TiO_2$  to hydrogenated  $TiO_2$ , which can

prevent the destruction of the pristine morphology of  $TiO_2$  nanotube arrays. The results show that the designed core/shell structure can not only improve the stability of hydrogenated  $TiO_2$  nanotube arrays through the ultrathin carbon coating but also enhance the separation of photogenerated electron-hole pairs due to the existence of a heterojunction interface. Furthermore, the highly conductive and active N-doped carbon thin film derived from MLD coating can significantly enhance the photoelectrochemical water splitting performances, which has a 5 time higher photocurrent and enhanced photostability than the original  $TiO_2$ .

Besides the most popular  $TiO_2$ -based catalysts, their group has further developed a MLD-assisted approach for the synthesis of Cu-ZnO catalysts used in the hydrogenation of levulinic acid to produce  $\gamma$ -valerolactone.<sup>105</sup> The Zn-hybrid film is deposited using a four-step (ABCB) MLD process, in which A, B, and C correspond to  $Zn(Et)_2$ , 1,4-phenylene diisocyanate (PPDI), and EDA. Similarly to  $TiO_2$ , the distance between moieties in the Cu-ZnO coating could be tuned by controlling the length of the

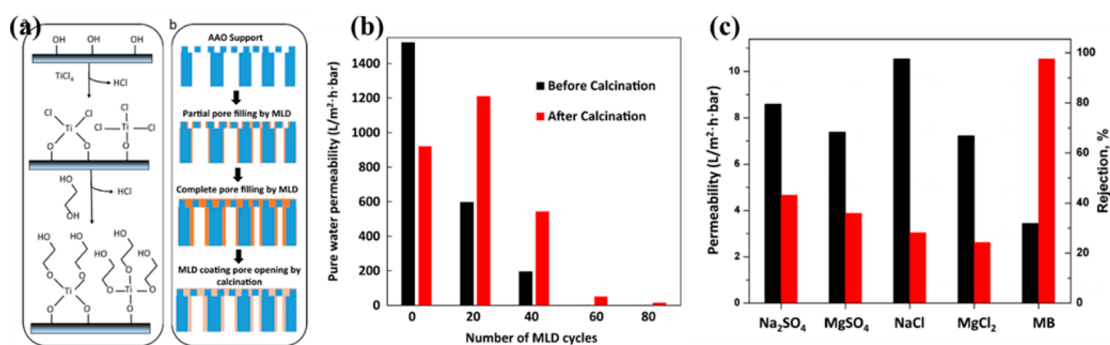


**Figure 10.** (a) Schematic diagrams of MLD surface reactions for titanium alkoxide coating growth using  $\text{TiCl}_4$  and EG as precursors; (b) pure water permeation through AAO with different cycles of MLD coatings before and after calcination at  $250\text{ }^\circ\text{C}$ ; (c) permeation through the AAO-60 $\text{TiO}_2$  membrane (black bar) and rejection of the AAO-60 $\text{TiO}_2$  membrane (red bar) (Copyright Elsevier, reproduced with permission from ref 108).

organic linkers. The catalysts display enhanced selectivity, efficiency, and stability due to the designed Cu–ZnO interface sites ( $\text{Cu}^0\text{Zn}$ ) and the synergistic effects between  $\text{Cu}^0\text{Zn}$  and  $\text{Cu}^+$ . Meanwhile, the ratio of  $\text{Cu}^0\text{Zn}$  sites could be simply controlled by adjusting the MLD cycles. This work provides a deeper understanding of the relationship between catalytic activity and the ratio of different Cu species ( $\text{Cu}^0\text{Zn}$ ,  $\text{Cu}^0$ , and  $\text{Cu}^+$ ), suggesting that the main active site is responsible for the remarkably enhanced catalytic activity and low activation energy.

In another study, Gregory's group designed  $\sim 20\text{ nm}$  thick poly(3,4-ethylenedioxythiophene) (PEDOT) films incorporated in high-conductivity mesoporous indium tin oxide (m-ITO) by a modified oxidative molecular layer deposition (oMLD).<sup>106</sup> Figure 9a illustrates a schematic diagram for the cathode electrode fabrication process of dye-sensitized solar cells (DSSCs). In the typical process, the  $\text{MoCl}_5$  vapor is first pulsed into the spin-cast m-ITO films and adsorbed on the surface of it. After purging to remove the unreacted  $\text{MoCl}_5$ , EDOT vapor is then introduced to the surface, leading to polymerization and formation of PEDOT films on the m-ITO, followed by purging of the HCl byproduct and excess EDOT. The growth rate of this oMLD PEDOT film is determined as  $1\text{ nm}$  per cycle at  $100\text{ }^\circ\text{C}$ . The 3D conductive/catalytic network has been successfully carried out as Pt-free cathodes for DSSCs with an open-circuit voltage equivalent to that of Pt cathode devices. The results show that PEDOT-coated m-ITO by oMLD possesses a power conversion efficiency of 7.18%, which is comparable to the 7.26% of Pt and higher than that of planar PEDOT coatings (4.85%). It is believed that the PEDOT deposited by oMLD can achieve high catalytic activities using more cost-effective and earth-abundant materials. This novel method can be extended to high-performance cathodes in other advanced photo- and electro-catalytic devices such as photoelectrochemical and fuel cell systems.

Methane reforming has received increasing attention in the past years, in which the reforming of methane (DRM) is used much less than methane steam reforming (MSR) due to its lower  $\text{H}_2/\text{CO}$  ratio and exacerbated issues with deactivation from coking. In this reaction, supported Ni is one of the most popular catalysts for DRM and MSR. To prevent the sintering of  $\sim 5\text{ nm}$  supported Ni particles during DRM, MLD alucone coatings with porous alumina can be used to stabilize the catalysts.<sup>107</sup> The uncoated catalyst is continuously deactivated during DRM at  $973\text{ K}$ . However, the DRM rates for the alucone-coated catalysts increase first before stabilizing, which is consistent with an increase of the nickel surface area when exposure to high

temperatures. Postreaction particles are relatively smaller for the MLD-coated catalysts. Catalysts with only five MLD layers had higher DRM rates than the uncoated catalyst, and a sample with 10 MLD layers can be very stable for 108 h.<sup>107</sup>

To summarize, there are very few reports focusing on MLD in the application of catalysis due to the early stages of MLD study. Similar to the field of energy storage, one of the effective strategies is to use MLD thin films as a template to fabricate N-doped carbon or porous metal oxide films, which can significantly enhance the catalytic performances. Another useful approach is to deposit highly conductive polymer films by ALD with high catalytic activities to replace the rare and expensive Pt. Finally, MLD thin films can also act as a support or stabilized coating for catalysts in some specific applications, like dry reforming of methane, which can effectively lengthen the lifetime of the pristine catalyst.

**MLD for Membrane Applications.** Water deficiency is another serious issue in many countries because of the increasing water use and depletion of usable fresh water resources. Nanofiltration membranes are widely considered for use in purifying drinking water and wastewater treatment, as well as pretreatment for desalination because of their ability to remove viruses, hardness, dissolved organic matter, and salts, especially multivalent ions. Among the possible nanofiltration membranes, ceramic nanofiltration membranes, usually manufactured from  $\text{Al}_2\text{O}_3$ ,  $\text{ZrO}_2$ , and  $\text{TiO}_2$ , have good chemical, thermal, and mechanical stability and a long lifetime under extreme operating conditions. For this type of membrane, the most important factor is the pore size, which is difficult to control at the nanometer level. In this case, MLD is an ideal method to deposit porous materials, including  $\text{Al}_2\text{O}_3$ ,  $\text{ZnO}$ ,  $\text{TiO}_2$ ,  $\text{SiO}_2$ , etc. Yu's group demonstrated MLD using  $\text{TiCl}_4$  and EG as precursors to deposit a titanium alkoxide coating on an anodic aluminum oxide (AAO) support (as shown in Figure 10a).<sup>108</sup> Further calcination is applied to obtain the microporous  $\text{TiO}_2$  coating on a mesoporous support. Different MLD coating thicknesses of 20, 40, 60, and 80 cycles have also been attempted to achieve the best performances. Figure 10b shows the water permeability through a bare AAO support and MLD coating AAO support (before and after calcination). The results show that the film derived from 60 MLD cycles formed a defect-free and dense Ti-EG MLD coating, which has a high pure water permeability of  $48\text{ L}/(\text{m}^2\text{h bar})$  after calcination at  $250\text{ }^\circ\text{C}$  in air. Moreover, the water purification performance of AAO-60 $\text{TiO}_2$  nanofiltration membranes has also been investigated for aqueous solutions of  $\text{NaCl}$ ,  $\text{Na}_2\text{SO}_4$ ,  $\text{MgCl}_2$ , and  $\text{MgSO}_4$  (as shown in Figure 10c). The results indicate that

AAO-60TiO<sub>2</sub> has high rejection for MB and natural organic matter (NOM), moderate rejection for salts, and good antifouling performance as well as recovery capability. It is believed that MLD will become a novel approach in the future for preparing metal oxide nanofiltration membranes with well-controlled thickness, composition, and membrane pore sizes.

Another group has introduced MLD for the deposition of PI at a low temperature of 110 °C for membrane separation.<sup>109</sup> It was found that globular PI is grown on both the free surface and pore walls of the polypropylene (PP) membranes. The results indicate that the PI-modified PP membranes display synergistically improved performances in various aspects, including the evidently enhanced surface hydrophilicity and permeation performance. Meanwhile, the overall separation efficiency is 85% higher even after 250 MLD cycles. Furthermore, the thermal stability of the PI-deposited PP membrane has also been improved, and the integrity of the porous structure has been well preserved after harsh treatments.

The MLD film plays an important role in stabilization of the SEI layer for both Li and Na metal anodes.

In this section, the present achievements of MLD in the application of membranes have been summarized. On one hand, the metal-containing MLD (metalcone) is considered to be a novel and effective method for the modification of nanofiltration membranes with postdeposition treatments. Additionally, polymer-based MLD can be used for membrane separation with improved surface hydrophilicity, permeation, separation efficiency, and thermal stability.

**Summary.** In summary, we have provided insight into the development and understanding of MLD in energy-related applications, and we also summarize the reported MLD films and the materials derived from MLD for the energy-related applications in Table 1. As shown in Figure 11, the MLD thin film can be generally separated into two types: one is the pure polymer thin films, and another one is the organic–inorganic

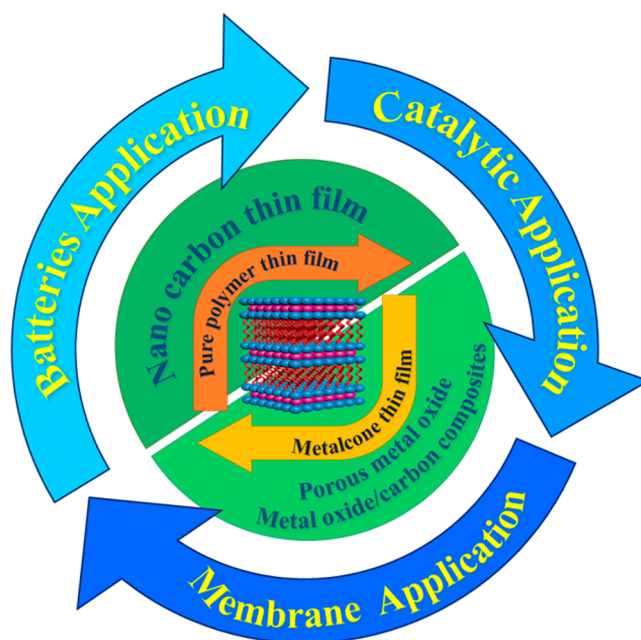


Figure 11. Schematic and summary of MLD thin films for the energy-related applications.

metalcone thin films. Furthermore, with post-treatments, different products will be achieved under different conditions, including nanocarbon thin films, porous metal oxide thin films, and metal oxide/carbon composites thin films. All of these films, including the original MLD films and films derived from MLD, display their own properties in the different applications.

The strategies for employing MLD for batteries and supercapacitors can be separated into two categories: (1) the direct use of MLD for electrodes and (2) the application of MLD for coating layers for electrode materials. Both the pristine MLD thin films and inorganic thin films derived from MLD yield excellent electrochemical performances and are very promising for battery and supercapacitor applications. Meanwhile, this

Table 1. Summary of MLD Thin Films and the Materials Derived from MLD Thin Films for the Energy-Related Applications

MLD thin film	precursors	materials derived from MLD	applications	refs
LiTP)	ti(thd) and terephthalic acid	–	electrode for LIBs	60
titanicones	TiCl <sub>4</sub> and EG	TiO <sub>2</sub> /carbon composites	electrode for LIBs	72
aromatic PI	PMDA and ODA	N-doped carbon coating on graphene	electrode for supercapacitor	61
alucone	TMA, GLY	–	surface coating for Si anode	75, 85, 86
alucone	TMA, HQ	–	surface coating for Si anode	76
alucone	TMA, EG	–	surface coating for Li metal anode	110
alucone	TMA, EG	–	surface coating for Na metal anode	97
alucone	TMA, EG	–	surface coating for C/S cathode	100
alucone	TMA, EG	–	surface coating for C/S cathode	101
titanicones	TiCl <sub>4</sub> and EG	TiO <sub>2</sub> /carbon composites	photocatalysis	104
Ti-hybrid film	TiCl <sub>4</sub> , EA and MC	N-doped TiO <sub>2</sub> nanoporous films	photocatalysis	38
–	PMDA and EDA	carbon-coated TiO <sub>2</sub> nanotube arrays	photoelectrochemical water splitting	103
Zn-hybrid film	Zn(Et) <sub>2</sub> , PPDI, EDA	Cu–ZnO	catalysts used in the hydrogenation of levulinic acid to produce $\gamma$ -valerolactone	105
PEDOT	EDOT, MoCl <sub>3</sub>	–	cathode electrode for DSSCs	106
alucone	TMA, EA, MA	porous alumina	stabilize the Ni catalysts	107
titanicones	TiCl <sub>4</sub> and EG	titanium alkoxide	modification of nanofiltration membranes	108
PI	PMDA, EDA	–	modification of PP membranes	109

unique gas-phase deposition method can be further used for all-solid-state batteries and flexible energy storage devices. Furthermore, MLD protective coating layers with high mechanical strength and flexibility have been shown to be ideal for electrodes with large volumetric expansions, including Si-, Li-, and S-based materials, leading to significantly improved electrochemical performances, stability, and lifetime. Thus, the MLD thin film can be an excellent candidate for energy storage applications, especially for batteries and supercapacitors.

Second, the field of energy conversion is also facing significant challenges in terms of catalysis. One of the effective methods for energy conversion is to use MLD thin films as templates to fabricate N-doped carbon or porous metal oxide materials, which can significantly enhance catalytic performance. Another useful approach is to deposit highly conductive polymer films by ALD with high catalytic activities to replace the conventionally used and expensive Pt. In addition, MLD thin films can also be considered as catalyst supports or stabilizing coatings in some specific applications, like dry reforming of methane, which can effectively lengthen the lifetime of the pristine catalyst.

Finally, we have shown that MLD can be utilized for membrane applications where controlled thickness, composition, and membrane pore sizes are needed, like nanofiltration and PP membranes. The MLD thin film can greatly improve surface hydrophilicity, permeation, separation efficiency, and thermal stability of membrane materials.

*Perspectives.* Although there are already some literature reporting different types of MLD coatings, the application of MLD in the field of energy storage and conversion is still in its infancy. More efforts should be focused on the development and application of novel MLD thin films. It is believed that the exploration and development of new MLD thin films should be targeting specific applications due to the unique requirements of each system. We propose to develop different classes of MLD materials for energy-related applications: (1) MLD is one ideal technique for the fabrication of electrodes for thin-film LIBs and 3D microbatteries. However, most reported MLD thin films (including metalcone and organic) are electrochemically inactive. In this case, the development of electrochemically active MLD thin films with high reversible capacity for batteries or supercapacitors is urgent. A novel MLD process with redox properties is expected to present higher reversible capacity for alkali ion intercalation/deintercalation. (2) Another aspect is to develop MLD thin films with high ionic conductivity (like Li (alkali ion)-containing MLD thin films), which can be used as the polymer-based solid-state electrolyte for all-solid-state batteries. (3) Highly conductive and catalytically active MLD thin films are used as catalysts for electrocatalytic devices. (4) More importantly, the MLD thin films are considered to be excellent candidates as surface coatings for the electrodes of LIBs and NIBs. However, new MLD coating development is still a big challenge, in which each purpose should correspond to each design for MLD coating. First, there are still no reports on the application of MLD thin films as surface coatings for the cathode materials of LIBs and NIBs. Facing this challenge, the MLD film with a wide electrochemical window, particularly at high voltage, is expected to be developed for surface modification for the cathode materials. Second, two big issues for alloy-based anodes (like Sn and Si) are relatively low conductivity and serious volume expansion. In order to solve these problems, new MLD coatings for Si should focus on developing conductive polymer MLD, like PANI, PPy, or PEDOT, and highly flexible MLD, like self-healing polymers. Third, the novel MLD films without any

decomposition at low electrochemical potential will be a good choice for the alkali metal anode to form a stable SEI layer and achieve reduced dendrite growth during the electrochemical plating/stripping process. (5) Hybrid thin films deposited combining ALD and MLD with layer-by-layer organic-inorganic structure or a more complex sandwich structure with the same concept will be more promising as the coating layer for electrode materials in battery applications, which inherited both advantages from both ALD and MLD.

As another important part of MLD, the development of nanomaterials or thin films derived from MLD is another field of interest for energy applications. (1) Although post-treatment (including H<sub>2</sub>O, air, and inert gases) is a facile and promising way method for MLD thin films, few works focus on applying MLD-derived materials for batteries and supercapacitors. It is believed that metal oxide thin films or metal oxide/carbon composite films are also promising as electrodes for energy-related applications. (2) Control over pore size and carbon content derived from metalcones should be further exploited for catalysts and membranes. (3) Furthermore, heteroatom-doped (N, S, and P) or co-doped carbon layers can be achieved by proper selection of the MLD precursors.

Thus, with continued efforts, MLD-based techniques can offer many solutions to address the current problems in the area of energy storage and conversion. The employment of MLD in energy applications deserves significant investigation in future studies to realize the maximum potential of this novel and versatile technique.

## ■ AUTHOR INFORMATION

### Corresponding Author

\*E-mail: [xsun@eng.uwo.ca](mailto:xsun@eng.uwo.ca).

### ORCID

Yang Zhao: 0000-0002-4148-2603

Xueliang Sun: 0000-0003-2881-8237

### Notes

The authors declare no competing financial interest.

### Biographies

**Yang Zhao** is currently a Ph.D. candidate in Prof. Xueliang (Andy) Sun's Group at the University of Western Ontario, Canada. He received his B.S. degree and M.S. degree from Northwestern Polytechnical University in 2011 and 2014, respectively. His current research interests focus on atomic/molecular layer deposition in the application of lithium/sodium ion batteries and all-solid-state batteries.

**Prof. Xueliang (Andy) Sun** is a Canada Research Chair in Development of Nanomaterials for Clean Energy, Fellow of the Royal Society of Canada and Canadian Academy of Engineering, and Full Professor at the University of Western Ontario, Canada. Dr. Sun received his Ph.D. in materials chemistry in 1999 from the University of Manchester, U.K., which he followed up by working as a postdoctoral fellow at the University of British Columbia, Canada and as a Research Associate at L'Institut National de la Recherche Scientifique (INRS), Canada. His current research interests are focused on advanced materials for electrochemical energy storage and conversion, including electrocatalysis in fuel cells and electrodes in lithium-ion batteries and metal-air batteries.

## ■ ACKNOWLEDGMENTS

This research was supported by the Natural Science and Engineering Research Council of Canada (NSERC), the Canada Research Chair Program (CRC), the Canada Foundation for

Innovation (CFI), and the University of Western Ontario (UWO). We gratefully acknowledge Mr. Keegan Adair for his help in the discussion and English polishing for this paper.

## REFERENCES

- (1) Wang, S.; Kang, Y.; Wang, L.; Zhang, H.; Wang, Y.; Wang, Y. Organic/inorganic hybrid sensors: a review. *Sens. Actuators, B* **2013**, *182*, 467–481.
- (2) Kaushik, A.; Kumar, R.; Arya, S. K.; Nair, M.; Malhotra, B. D.; Bhansali, S. Organic-inorganic hybrid nanocomposite-based gas sensors for environmental monitoring. *Chem. Rev.* **2015**, *115*, 4571–606.
- (3) Leng, C. Z.; Losego, M. D. Vapor phase infiltration (VPI) for transforming polymers into organic-inorganic hybrid materials: a critical review of current progress and future challenges. *Mater. Horiz.* **2017**, *4*, 747–771.
- (4) Um, H. D.; Choi, D.; Choi, A.; Seo, J. H.; Seo, K. Embedded metal electrode for organic-inorganic hybrid nanowire solar cells. *ACS Nano* **2017**, *11*, 6218–6224.
- (5) Sundberg, P.; Karppinen, M. Organic and inorganic-organic thin film structures by molecular layer deposition: A review. *Beilstein J. Nanotechnol.* **2014**, *5*, 1104–36.
- (6) Lee, B. H.; Yoon, B.; Abdulgatov, A. I.; Hall, R. A.; George, S. M. Growth and properties of hybrid organic-inorganic metalcone films using molecular layer deposition techniques. *Adv. Funct. Mater.* **2013**, *23*, 532–546.
- (7) Rahman, M.; Davey, K.; Qiao, S.-Z. Advent of 2D rhenium disulfide (ReS<sub>2</sub>): fundamentals to applications. *Adv. Funct. Mater.* **2017**, *27*, 1606129.
- (8) Ran, J.; Gao, G.; Li, F. T.; Ma, T. Y.; Du, A.; Qiao, S. Z. Ti<sub>3</sub>C<sub>2</sub> MXene co-catalyst on metal sulfide photo-absorbers for enhanced visible-light photocatalytic hydrogen production. *Nat. Commun.* **2017**, *8*, 13907.
- (9) Ran, J.; Zhu, B.; Qiao, S. Z. Phosphorene Co-catalyst advancing highly efficient visible-light photocatalytic hydrogen production. *Angew. Chem., Int. Ed.* **2017**, *56*, 10373–10377.
- (10) Ran, J.; Jaroniec, M.; Qiao, S. Z. Cocatalysts in semiconductor-based photocatalytic CO<sub>2</sub> reduction: achievements, challenges, and opportunities. *Adv. Mater.* **2018**, *30*, 1704649.
- (11) Kango, S.; Kalia, S.; Celli, A.; Njuguna, J.; Habibi, Y.; Kumar, R. Surface modification of inorganic nanoparticles for development of organic-inorganic nanocomposites-A review. *Prog. Polym. Sci.* **2013**, *38*, 1232–1261.
- (12) Figueira, R. B.; Silva, C. J. R.; Pereira, E. V. Organic-inorganic hybrid sol-gel coatings for metal corrosion protection: a review of recent progress. *J. Coat. Technol. Res.* **2015**, *12*, 1–35.
- (13) Dong, X.; Zhuo, X.; Wei, J.; Zhang, G.; Li, Y. Wood-based nanocomposite derived by in situ formation of organic-inorganic hybrid polymer within wood via a sol-gel method. *ACS Appl. Mater. Interfaces* **2017**, *9*, 9070–9078.
- (14) Liu, J.; Sun, X. Elegant design of electrode and electrode/electrolyte interface in lithium-ion batteries by atomic layer deposition. *Nanotechnology* **2015**, *26*, 024001.
- (15) Gao, Z.; Qin, Y. Design and Properties of confined nanocatalysts by atomic layer deposition. *Acc. Chem. Res.* **2017**, *50*, 2309–2316.
- (16) Meng, X. Atomic-scale surface modifications and novel electrode designs for high-performance sodium-ion batteries via atomic layer deposition. *J. Mater. Chem. A* **2017**, *5*, 10127–10149.
- (17) Meng, X.; Wang, X.; Geng, D.; Ozgit-Akgun, C.; Schneider, N.; Elam, J. W. Atomic layer deposition for nanomaterial synthesis and functionalization in energy technology. *Mater. Horiz.* **2017**, *4*, 133–154.
- (18) Yoshimura, T.; Tatsuura, S.; Sotoyama, W. Polymer films formed with monolayer growth steps by molecular layer deposition. *Appl. Phys. Lett.* **1991**, *59*, 482–484.
- (19) Yoshimura, T.; Tatsuura, S.; Sotoyama, W.; Matsuura, A.; Hayano, T. Quantum wire and dot formation by chemical vapor deposition and molecular layer deposition of one-dimensional conjugated polymer. *Appl. Phys. Lett.* **1992**, *60*, 268–270.
- (20) Du, Y.; George, S. M. Molecular layer deposition of nylon 66 films examined using in situ FTIR spectroscopy. *J. Phys. Chem. C* **2007**, *111*, 8509–8517.
- (21) Adamczyk, N. M.; Dameron, A. A.; George, S. M. Molecular layer deposition of poly(p-phenylene terephthalamide) films using terephthaloyl chloride and p-phenylenediamine. *Langmuir* **2008**, *24*, 2081–2089.
- (22) George, S. M.; Yoon, B.; Dameron, A. A. Surface chemistry for molecular layer deposition of organic and hybrid organic-inorganic polymers. *Acc. Chem. Res.* **2009**, *42*, 498–508.
- (23) Loscutoff, P. W.; Lee, H.-B.-R.; Bent, S. F. Deposition of ultrathin polythiourea films by molecular layer deposition. *Chem. Mater.* **2010**, *22*, 5563–5569.
- (24) Loscutoff, P. W.; Zhou, H.; Clendinning, S. B.; Bent, S. F. Formation of organic nanoscale laminates and blends by molecular layer deposition. *ACS Nano* **2010**, *4*, 331–341.
- (25) Peng, Q.; Efimenko, K.; Genzer, J.; Parsons, G. N. Oligomer orientation in vapor-molecular-layer-deposited alkyl-aromatic polyamide films. *Langmuir* **2012**, *28*, 10464–70.
- (26) Zhou, W.; Leem, J.; Park, I.; Li, Y.; Jin, Z.; Min, Y.-S. Charge trapping behavior in organic-inorganic alloy films grown by molecular layer deposition from trimethylaluminum, p-phenylenediamine and water. *J. Mater. Chem.* **2012**, *22*, 23935.
- (27) Zhou, H.; Toney, M. F.; Bent, S. F. Cross-linked ultrathin polyurea films via molecular layer deposition. *Macromolecules* **2013**, *46*, 5638–5643.
- (28) Park, Y. S.; Choi, S. E.; Kim, H.; Lee, J. S. Fine-tunable absorption of uniformly aligned polyurea thin films for optical filters using sequentially self-limited molecular layer deposition. *ACS Appl. Mater. Interfaces* **2016**, *8*, 11788–95.
- (29) Bahlawane, N.; Arl, D.; Thomann, J.-S.; Adjeroud, N.; Menguelti, K.; Lenoble, D. Molecular layer deposition of amine-containing alucone thin films. *Surf. Coat. Technol.* **2013**, *230*, 101–105.
- (30) Dameron, A. A.; Seghete, D.; Burton, B. B.; Davidson, S. D.; Cavanagh, A. S.; Bertrand, J. A.; George, S. M. Molecular layer deposition of alucone polymer films using trimethylaluminum and ethylene glycol. *Chem. Mater.* **2008**, *20*, 3315–3326.
- (31) Choudhury, D.; Sarkar, S. K.; Mahuli, N. Molecular layer deposition of alucone films using trimethylaluminum and hydroquinone. *J. Vac. Sci. Technol., A* **2015**, *33*, 01A115.
- (32) Park, Y. S.; Kim, H.; Cho, B.; Lee, C.; Choi, S. E.; Sung, M. M.; Lee, J. S. Intramolecular and intermolecular interactions in hybrid organic-inorganic alucone films grown by molecular layer deposition. *ACS Appl. Mater. Interfaces* **2016**, *8*, 17489–98.
- (33) Van de Kerckhove, K.; Mattelaer, F.; Dendooven, J.; Detavernier, C. Molecular layer deposition of "vanadicone", a vanadium-based hybrid material, as an electrode for lithium-ion batteries. *Dalton Trans.* **2017**, *46*, 4542–4553.
- (34) Ahvenniemi, E.; Karppinen, M. ALD/MLD processes for Mn and Co based hybrid thin films. *Dalton Trans.* **2016**, *45*, 10730–5.
- (35) Vähä-Nissi, M.; Sundberg, P.; Kauppi, E.; Hirvikorpi, T.; Sievänen, J.; Sood, A.; Karppinen, M.; Harlin, A. Barrier properties of Al<sub>2</sub>O<sub>3</sub> and alucone coatings and nanolaminates on flexible biopolymer films. *Thin Solid Films* **2012**, *520*, 6780–6785.
- (36) Choudhury, D.; Sarkar, S. K.; Mahuli, N. Molecular layer deposition of alucone films using trimethylaluminum and hydroquinone. *J. Vac. Sci. Technol., A* **2015**, *33*, 01A115–3.
- (37) Lee, B. H.; Yoon, B.; Anderson, V. R.; George, S. M. Alucone alloys with tunable properties using alucone molecular layer deposition and Al<sub>2</sub>O<sub>3</sub> atomic layer deposition. *J. Phys. Chem. C* **2012**, *116*, 3250–3257.
- (38) Chen, C.; Li, P.; Wang, G.; Yu, Y.; Duan, F.; Chen, C.; Song, W.; Qin, Y.; Knez, M. Nanoporous nitrogen-doped titanium dioxide with excellent photocatalytic activity under visible light irradiation produced by molecular layer deposition. *Angew. Chem., Int. Ed.* **2013**, *52*, 9196–200.
- (39) Ghazaryan, L.; Kley, E.-B.; Tünnemann, A.; Viorica Szeghalmi, A. Stability and annealing of alucones and alucone alloys. *J. Vac. Sci. Technol., A* **2013**, *31*, 01A149.

- (40) Lee, B. H.; Anderson, V. R.; George, S. M. Metalcone and metalcone/metal oxide alloys grown using atomic & molecular layer deposition. *ECS Trans.* **2011**, *41*, 131–138.
- (41) Zhou, H.; Bent, S. F. Fabrication of organic interfacial layers by molecular layer deposition: Present status and future opportunities. *J. Vac. Sci. Technol., A* **2013**, *31*, 040801.
- (42) Leskelä, M.; Ritala, M.; Nilsen, O. Novel materials by atomic layer deposition and molecular layer deposition. *MRS Bull.* **2011**, *36*, 877–884.
- (43) Meng, X. An overview of molecular layer deposition for organic and organic–inorganic hybrid materials: mechanisms, growth characteristics, and promising applications. *J. Mater. Chem. A* **2017**, *5*, 18326–18378.
- (44) Van Bui, H.; Grillo, F.; van Ommen, J. R. Atomic and molecular layer deposition: off the beaten track. *Chem. Commun.* **2017**, *53*, 45–71.
- (45) Ma, L.; Nuwayhid, R. B.; Wu, T.; Lei, Y.; Amine, K.; Lu, J. Atomic layer deposition for lithium-based batteries. *Adv. Mater. Interfaces* **2016**, *3*, 1600564.
- (46) Gregorczyk, K.; Knez, M. Hybrid nanomaterials through molecular and atomic layer deposition: Top down, bottom up, and in-between approaches to new materials. *Prog. Mater. Sci.* **2016**, *75*, 1–37.
- (47) Yoshimura, T.; Oshima, A.; Kim, D.; Morita, Y. Quantum dot formation in polymer wires by three-molecule molecular layer deposition (MLD) and applications to electro-optic/photovoltaic devices. *ECS Trans.* **2009**, *25*, 15–25.
- (48) Li, Y. H.; Wang, D.; Buriak, J. M. Molecular layer deposition of thiol-ene multilayers on semiconductor surfaces. *Langmuir* **2010**, *26*, 1232–8.
- (49) Yoshimura, T.; Ebihara, R.; Oshima, A. Polymer wires with quantum dots grown by molecular layer deposition of three source molecules for sensitized photovoltaics. *J. Vac. Sci. Technol., A* **2011**, *29*, 051510.
- (50) Zhou, H.; Bent, S. F. Molecular layer deposition of functional thin films for advanced lithographic patterning. *ACS Appl. Mater. Interfaces* **2011**, *3*, 505–11.
- (51) Yoshimura, T.; Ishii, S. Effect of quantum dot length on the degree of electron localization in polymer wires grown by molecular layer deposition. *J. Vac. Sci. Technol., A* **2013**, *31*, 031501.
- (52) Zhao, Y.; Li, X.; Yan, B.; Xiong, D.; Li, D.; Lawes, S.; Sun, X. Recent developments and understanding of novel mixed transition-metal oxides as anodes in lithium ion batteries. *Adv. Energy Mater.* **2016**, *6*, 1502175.
- (53) Zhao, Y.; Song, Z.; Li, X.; Sun, Q.; Cheng, N.; Lawes, S.; Sun, X. Metal organic frameworks for energy storage and conversion. *Energy Storage Materials* **2016**, *2*, 35–62.
- (54) Zhao, Y.; Li, X.; Yan, B.; Li, D.; Lawes, S.; Sun, X. Significant impact of 2D graphene nanosheets on large volume change tin-based anodes in lithium-ion batteries: A review. *J. Power Sources* **2015**, *274*, 869–884.
- (55) Ban, C.; George, S. M. Molecular layer deposition for surface modification of lithium-ion battery electrodes. *Adv. Mater. Interfaces* **2016**, *3*, 1600762.
- (56) Xiao, B.; Liu, J.; Sun, Q.; Wang, B.; Banis, M. N.; Zhao, D.; Wang, Z.; Li, R.; Cui, X.; Sham, T. K.; Sun, X. Unravelling the role of electrochemically active FePO<sub>4</sub> coating by atomic layer deposition for increased high-voltage stability of LiNi<sub>0.5</sub>Mn<sub>1.5</sub>O<sub>4</sub> cathode material. *Adv. Sci.* **2015**, *2*, 1500022.
- (57) Li, X.; Liu, J.; Banis, M. N.; Lushington, A.; Li, R.; Cai, M.; Sun, X. Atomic layer deposition of solid-state electrolyte coated cathode materials with superior high-voltage cycling behavior for lithium ion battery application. *Energy Environ. Sci.* **2014**, *7*, 768–778.
- (58) Xie, J.; Sendek, A. D.; Cubuk, E. D.; Zhang, X.; Lu, Z.; Gong, Y.; Wu, T.; Shi, F.; Liu, W.; Reed, E. J.; Cui, Y. Atomic layer deposition of stable LiAlF<sub>4</sub> lithium ion conductive interfacial layer for stable cathode cycling. *ACS Nano* **2017**, *11*, 7019–7027.
- (59) Meng, X.; Yang, X. Q.; Sun, X. Emerging applications of atomic layer deposition for lithium-ion battery studies. *Adv. Mater.* **2012**, *24*, 3589–615.
- (60) Nisula, M.; Karppinen, M. Atomic/molecular layer deposition of lithium terephthalate thin films as high rate capability Li-ion battery anodes. *Nano Lett.* **2016**, *16*, 1276–81.
- (61) Chen, Y.; Gao, Z.; Zhang, B.; Zhao, S.; Qin, Y. Graphene coated with controllable N-doped carbon layer by molecular layer deposition as electrode materials for supercapacitors. *J. Power Sources* **2016**, *315*, 254–260.
- (62) Liu, J.; Meng, X.; Banis, M. N.; Cai, M.; Li, R.; Sun, X. Crystallinity-controlled synthesis of zirconium oxide thin films on nitrogen-doped carbon nanotubes by atomic layer deposition. *J. Phys. Chem. C* **2012**, *116*, 14656–14664.
- (63) Li, X.; Meng, X.; Liu, J.; Geng, D.; Zhang, Y.; Banis, M. N.; Li, Y.; Yang, J.; Li, R.; Sun, X.; Cai, M.; Verbrugge, M. W. Tin oxide with controlled morphology and crystallinity by atomic layer deposition onto graphene nanosheets for enhanced lithium storage. *Adv. Funct. Mater.* **2012**, *22*, 1647–1654.
- (64) Meng, X.; Geng, D.; Liu, J.; Li, R.; Sun, X. Controllable synthesis of graphene-based titanium dioxide nanocomposites by atomic layer deposition. *Nanotechnology* **2011**, *22*, 165602.
- (65) Liu, J.; Banis, M. N.; Li, X.; Lushington, A.; Cai, M.; Li, R.; Sham, T.-K.; Sun, X. Atomic layer deposition of lithium tantalate solid-state electrolytes. *J. Phys. Chem. C* **2013**, *117*, 20260–20267.
- (66) Liu, J.; Tang, Y.; Xiao, B.; Sham, T.-K.; Li, R.; Sun, X. Atomic layer deposited aluminium phosphate thin films on N-doped CNTs. *RSC Adv.* **2013**, *3*, 4492.
- (67) Liu, J.; Banis, M. N.; Sun, Q.; Lushington, A.; Li, R.; Sham, T. K.; Sun, X. Rational design of atomic-layer-deposited LiFePO<sub>4</sub> as a high-performance cathode for lithium-ion batteries. *Adv. Mater.* **2014**, *26*, 6472–7.
- (68) Liu, J.; Banis, M. N.; Xiao, B.; Sun, Q.; Lushington, A.; Li, R.; Guo, J.; Sham, T.-K.; Sun, X. Atomically precise growth of sodium titanates as anode materials for high-rate and ultralong cycle-life sodium-ion batteries. *J. Mater. Chem. A* **2015**, *3*, 24281–24288.
- (69) Liu, J.; Xiao, B.; Banis, M. N.; Li, R.; Sham, T.-K.; Sun, X. Atomic layer deposition of amorphous iron phosphates on carbon nanotubes as cathode materials for lithium-ion batteries. *Electrochim. Acta* **2015**, *162*, 275–281.
- (70) Wang, B.; Liu, J.; Norouzi Banis, M.; Sun, Q.; Zhao, Y.; Li, R.; Sham, T. K.; Sun, X. Atomic layer deposited lithium silicates as solid-state electrolytes for all-solid-state batteries. *ACS Appl. Mater. Interfaces* **2017**, *9*, 31786–31793.
- (71) Wang, B.; Zhao, Y.; Banis, M. N.; Sun, Q.; Adair, K. R.; Li, R.; Sham, T. K.; Sun, X. Atomic layer deposition of lithium niobium oxides as potential solid-state electrolytes for lithium-ion batteries. *ACS Appl. Mater. Interfaces* **2018**, *10*, 1654–1661.
- (72) Van de Kerckhove, K.; Mattelaer, F.; Deduytsche, D.; Vereecken, P. M.; Dendooven, J.; Detavernier, C. Molecular layer deposition of “titanicone”, a titanium-based hybrid material, as an electrode for lithium-ion batteries. *Dalton Trans.* **2016**, *45*, 1176–84.
- (73) Abdulgatov, A. I.; Terauds, K. E.; Travis, J. J.; Cavanagh, A. S.; Raj, R.; George, S. M. Pyrolysis of titanicone molecular layer deposition films as precursors for conducting TiO<sub>2</sub>/carbon composite films. *J. Phys. Chem. C* **2013**, *117*, 17442–17450.
- (74) Lushington, A.; Liu, J.; Bannis, M. N.; Xiao, B.; Lawes, S.; Li, R.; Sun, X. A novel approach in controlling the conductivity of thin films using molecular layer deposition. *Appl. Surf. Sci.* **2015**, *357*, 1319–1324.
- (75) Piper, D. M.; Travis, J. J.; Young, M.; Son, S. B.; Kim, S. C.; Oh, K. H.; George, S. M.; Ban, C.; Lee, S. H. Reversible high-capacity Si nanocomposite anodes for lithium-ion batteries enabled by molecular layer deposition. *Adv. Mater.* **2014**, *26*, 1596–601.
- (76) Molina Piper, D.; Lee, Y.; Son, S.-B.; Evans, T.; Lin, F.; Nordlund, D.; Xiao, X.; George, S. M.; Lee, S.-H.; Ban, C. Cross-linked aluminum dioxymethylene coating for stabilization of silicon electrodes. *Nano Energy* **2016**, *22*, 202–210.
- (77) Wu, H.; Cui, Y. Designing nanostructured Si anodes for high energy lithium ion batteries. *Nano Today* **2012**, *7*, 414–429.
- (78) Chan, C. K.; Peng, H.; Liu, G.; McIlwrath, K.; Zhang, X. F.; Huggins, R. A.; Cui, Y. High-performance lithium battery anodes using silicon nanowires. *Nat. Nanotechnol.* **2008**, *3*, 31–5.

- (79) Wu, H.; Zheng, G.; Liu, N.; Carney, T. J.; Yang, Y.; Cui, Y. Engineering empty space between Si nanoparticles for lithium-ion battery anodes. *Nano Lett.* **2012**, *12*, 904–9.
- (80) Yao, Y.; Liu, N.; McDowell, M. T.; Pasta, M.; Cui, Y. Improving the cycling stability of silicon nanowire anodes with conducting polymer coatings. *Energy Environ. Sci.* **2012**, *5*, 7927.
- (81) Wang, C.; Wu, H.; Chen, Z.; McDowell, M. T.; Cui, Y.; Bao, Z. Self-healing chemistry enables the stable operation of silicon micro-particle anodes for high-energy lithium-ion batteries. *Nat. Chem.* **2013**, *5*, 1042–8.
- (82) Wu, H.; Yu, G.; Pan, L.; Liu, N.; McDowell, M. T.; Bao, Z.; Cui, Y. Stable Li-ion battery anodes by in-situ polymerization of conducting hydrogel to conformally coat silicon nanoparticles. *Nat. Commun.* **2013**, *4*, 1943.
- (83) Chen, Y.; Zeng, S.; Qian, J.; Wang, Y.; Cao, Y.; Yang, H.; Ai, X. Li(+)-conductive polymer-embedded nano-Si particles as anode material for advanced Li-ion batteries. *ACS Appl. Mater. Interfaces* **2014**, *6*, 3508–12.
- (84) Mohamed, S. G.; Tsai, Y. Q.; Chen, C. J.; Tsai, Y. T.; Hung, T. F.; Chang, W. S.; Liu, R. S. Ternary spinel MCoO (M = Mn, Fe, Ni, and Zn) porous nanorods as bifunctional cathode materials for lithium-O<sub>2</sub> batteries. *ACS Appl. Mater. Interfaces* **2015**, *7*, 12038–12046.
- (85) He, Y.; Piper, D. M.; Gu, M.; Travis, J. J.; George, S. M.; Lee, S. H.; Genc, A.; Pullan, L.; Liu, J.; Mao, S. X.; et al. In situ transmission electron microscopy probing of native oxide and artificial layers on silicon nanoparticles for lithium ion batteries. *ACS Nano* **2014**, *8*, 11816–11823.
- (86) Luo, L.; Yang, H.; Yan, P.; Travis, J. J.; Lee, Y.; Liu, N.; Molina Piper, D. M.; Zhang, S.; Ban, C.; Lee, S. H.; et al. Surface-coating regulated lithiation kinetics and degradation in silicon nanowires for lithium ion battery. *ACS Nano* **2015**, *9*, 5559–5566.
- (87) Ma, Y.; Martinez de la Hoz, J. M.; Angarita, I.; Berrio-Sanchez, J. M.; Benitez, L.; Seminario, J. M.; Son, S. B.; Lee, S. H.; George, S. M.; Ban, C.; et al. Structure and reactivity of alucone-coated films on Si and Li<sub>1</sub>Si<sub>y</sub> surfaces. *ACS Appl. Mater. Interfaces* **2015**, *7*, 11948–55.
- (88) Younesi, R.; Veith, G. M.; Johansson, P.; Edström, K.; Vegge, T. Lithium salts for advanced lithium batteries: Li-metal, Li-O<sub>2</sub>, and Li-S. *Energy Environ. Sci.* **2015**, *8*, 1905–1922.
- (89) Cheng, X.-B.; Zhang, R.; Zhao, C.-Z.; Wei, F.; Zhang, J.-G.; Zhang, Q. A review of solid electrolyte interphases on lithium metal anode. *Adv. Sci.* **2016**, *3*, 1500213.
- (90) Xu, W.; Wang, J.; Ding, F.; Chen, X.; Nasybulin, E.; Zhang, Y.; Zhang, J.-G. Lithium metal anodes for rechargeable batteries. *Energy Environ. Sci.* **2014**, *7*, 513–537.
- (91) Vaughney, J. T.; Liu, G.; Zhang, J.-G. Stabilizing the surface of lithium metal. *MRS Bull.* **2014**, *39*, 429–435.
- (92) Yang, C.; Fu, K.; Zhang, Y.; Hitz, E.; Hu, L. Protected lithium-metal anodes in batteries: from liquid to solid. *Adv. Mater.* **2017**, *29*, 1701169.
- (93) Xin, S.; You, Y.; Wang, S.; Gao, H.-C.; Yin, Y.-X.; Guo, Y.-G. Solid-state lithium metal batteries promoted by nanotechnology: progress and prospects. *ACS Energy Lett.* **2017**, *2*, 1385–1394.
- (94) Wood, K. N.; Noked, M.; Dasgupta, N. P. Lithium metal anodes: toward an improved understanding of coupled morphological, electrochemical, and mechanical behavior. *ACS Energy Lett.* **2017**, *2*, 664–672.
- (95) Kozen, A. C.; Lin, C. F.; Pearse, A. J.; Schroeder, M. A.; Han, X. G.; Hu, L. B.; Lee, S. B.; Rubloff, G. W.; Noked, M. Next-generation lithium metal anode engineering via atomic layer deposition. *ACS Nano* **2015**, *9*, 5884–5892.
- (96) Kazyak, E.; Wood, K. N.; Dasgupta, N. P. Improved cycle life and stability of lithium metal anodes through ultrathin atomic layer deposition surface treatments. *Chem. Mater.* **2015**, *27*, 6457–6462.
- (97) Zhao, Y.; Goncharova, L. V.; Zhang, Q.; Kaghazchi, P.; Sun, Q.; Lushington, A.; Wang, B.; Li, R.; Sun, X. Inorganic-organic coating via molecular layer deposition enables long life sodium metal anode. *Nano Lett.* **2017**, *17*, 5653–5659.
- (98) Zhao, Y.; Goncharova, L. V.; Lushington, A.; Sun, Q.; Yadegari, H.; Wang, B.; Xiao, W.; Li, R.; Sun, X. Superior stable and long life sodium metal anodes achieved by atomic layer deposition. *Adv. Mater.* **2017**, *29*, 1606663.
- (99) Luo, W.; Lin, C.-F.; Zhao, O.; Noked, M.; Zhang, Y.; Rubloff, G. W.; Hu, L. Ultrathin surface coating enables the stable sodium metal anode. *Adv. Energy Mater.* **2017**, *7*, 1601526.
- (100) Li, X.; Lushington, A.; Liu, J.; Li, R.; Sun, X. Superior stable sulfur cathodes of Li-S batteries enabled by molecular layer deposition. *Chem. Commun.* **2014**, *50*, 9757–60.
- (101) Li, X.; Lushington, A.; Sun, Q.; Xiao, W.; Liu, J.; Wang, B.; Ye, Y.; Nie, K.; Hu, Y.; Xiao, Q.; Li, R.; Guo, J.; Sham, T. K.; Sun, X. Safe and durable high-temperature lithium-sulfur batteries via molecular layer deposited coating. *Nano Lett.* **2016**, *16*, 3545–9.
- (102) Li, X.; Liu, J.; Wang, B.; Banis, M. N.; Xiao, B.; Li, R.; Sham, T.-K.; Sun, X. Nanoscale stabilization of Li–sulfur batteries by atomic layer deposited Al<sub>2</sub>O<sub>3</sub>. *RSC Adv.* **2014**, *4*, 27126.
- (103) Tong, X.; Yang, P.; Wang, Y.; Qin, Y.; Guo, X. Enhanced photoelectrochemical water splitting performance of TiO<sub>2</sub> nanotube arrays coated with an ultrathin nitrogen-doped carbon film by molecular layer deposition. *Nanoscale* **2014**, *6*, 6692–700.
- (104) Ishchuk, S.; Taffa, D. H.; Hazut, O.; Kaynan, N.; Yerushalmi, Y. Transformation of organic-inorganic hybrid films obtained by molecular layer deposition to photocatalytic layers with enhanced activity. *ACS Nano* **2012**, *6*, 7263–7269.
- (105) Zhang, B.; Chen, Y.; Li, J.; Pippel, E.; Yang, H.; Gao, Z.; Qin, Y. High efficiency Cu–ZnO hydrogenation catalyst: the tailoring of Cu–ZnO interface sites by molecular layer deposition. *ACS Catal.* **2015**, *5*, 5567–5573.
- (106) Kim, D. H.; Atanasov, S. E.; Lemaire, P.; Lee, K.; Parsons, G. N. Platinum-free cathode for dye-sensitized solar cells using poly(3,4-ethylenedioxythiophene) (PEDOT) formed via oxidative molecular layer deposition. *ACS Appl. Mater. Interfaces* **2015**, *7*, 3866–70.
- (107) Gould, T. D.; Izar, A.; Weimer, A. W.; Falconer, J. L.; Medlin, J. W. Stabilizing Ni catalysts by molecular layer deposition for harsh, dry reforming conditions. *ACS Catal.* **2014**, *4*, 2714–2717.
- (108) Song, Z.; Fathizadeh, M.; Huang, Y.; Chu, K. H.; Yoon, Y.; Wang, L.; Xu, W. L.; Yu, M. TiO<sub>2</sub> nanofiltration membranes prepared by molecular layer deposition for water purification. *J. Membr. Sci.* **2016**, *510*, 72–78.
- (109) Xiong, S.; Sheng, T.; Kong, L.; Zhong, Z.; Huang, J.; Wang, Y. Enhanced performances of polypropylene membranes by molecular layer deposition of polyimide. *Chin. J. Chem. Eng.* **2016**, *24*, 843–849.
- (110) Zhao, Y.; Goncharova, L. V.; Sun, Q.; Li, X.; Lushington, A.; Wang, B.; Li, R.; Dai, F.; Cai, M.; Sun, X. Robust metallic lithium anode protected by molecular layer deposition technique. *Small Methods* **2018**.